Journal of Catalysis 274 (2010) 29–51

Contents lists available at ScienceDirect

Journal of Catalysis

journal homepage: www.elsevier.com/locate/jcat

Acid strength of solids probed by catalytic isobutane conversion

Dan Fraenkel *, Nicholas R. Jentzsch, Christopher A. Starr [1], Pandurang V. Nikrad

Eltron Research & Development Inc., 4600 Nautilus Court South, Boulder, CO 80301, USA

ARTICLE INFO

Article history:
Received 25 September 2009
Revised 26 March 2010
Accepted 2 June 2010
Available online 22 July 2010

This work is dedicated to the late W. Keith Hall.

Keywords:
Hammett-acidity function
Isobutane conversion
Alkane isomerization
Alkane disproportionation
Hammett indicator
Zeolite
Sulfated zirconia
Brønsted acid

ABSTRACT

The literature is controversial on whether sulfated zirconia (SZ) is "just" as strong acid as H-zeolites, or a strong superacid. Spectroscopic studies of adsorbed probe molecules concluded that SZ is not a superacid, whereas acidity measurements based on Hammett indicators, alkane transformations and the 1/2% isobutane conversion test [B. Umansky, J. Engelhardt, W.K. Hall, J. Catal. 127 (1991) 128; D. Fraenkel, Chem. Lett. (1999) 917] indicated that SZ is superacidic. We for the first time applied direct acidity measurements under comparative conditions for SZ and common H-zeolites in a single series and found that the apparent acid strength order is SZ ($H_0 \sim -18$) $\gg$ HM (-14) > HZSM-5 (-10) $\approx$ HY (-9), in agreement with previous studies employing the zeolites and SZ separately. Product distribution at 1/2% isobutane conversion is in full agreement with the acid ranking and strength; SZ gives the typical pattern of known superacids (Magic Acid®, HCl–$AlCl_3$), whereas the weaker acid zeolites' pattern is consistent with that of other weaker acids.

1. Introduction

Probing acidity in strong solid acids allows ranking those acids by the extent of their strength and comparing them with liquid acids of similar strength. Such probing may also enhance our understanding of the effect of acidity on catalytic performance by clarifying the relationship between acid strength and mechanisms of acid-catalyzed organic reactions, e.g., hydrocarbon conversions. Acids extend about 20 orders of magnitude in terms of their reaction kinetic rates in catalytic processes; on the Hammett acidity scale, using the H_0 function, this corresponds to approximately -3 to -23. On such a scale, various acid strength ranges can be defined, such as -3 to -8 for "weak acids", -8 to -12 for "strong acids", and <-12 for "very strong acids", or superacids according to the 1971 definition of Gillespie and Peel [1] based on the strength of 100% H_2SO_4. Among the latter acids, fluorine-containing systems have been of most interest, and they were most thoroughly investigated [1,2]. However, the corrosiveness and toxicity of such systems, and more generally, of any halogen-containing acid, has limited their application in industrial processes in spite of their tremendous activity and efficiency in petroleum refining reactions and petrochemical conversions.

To become environmentally acceptable, a superacid catalyst should be non-corrosive and non-toxic; preferably, it should be a solid. Ideally, a solid superacid should be based on oxides or oxide mixtures of the simple, abundant, non-volatile and non-toxic elements. In 1980, Hino and Arata prepared [3] a sulfate-promoted tetragonal zirconia – later called sulfated zirconia (SZ) – by thermally treating a sulfuric acid washed oxy-hydroxy zirconium precipitated from a zirconium salt solution. They claimed, based on the Hammett indicator test, that SZ exhibits superacidity with $H_0 < -16$; in accord with this finding, SZ was shown active in the isomerization of *n*-butane and of *n*-pentane at ambient conditions. Soon after, other similarly sulfated metal oxides (e.g., of titanium, tin, hafnium) were also claimed to be superacidic by the above criteria [4]. Spectroscopic evidence that SZ has superacidic protons was reported by Riemer et al. [5] based on ^{1}H MAS NMR; they showed a broadened proton peak at δ 5.85, 1.5 ppm lower than the peak of the acidic proton of HZSM-5 (δ 4.3), a zeolite acid known to be strongly acidic.

The possibility that some sulfated metal oxides may form a new class of solid acids that are superacidic, and thus surpass the acidity of common solid acid systems, such as H-zeolites, urged many researchers to further investigate the above structures. During the 1990s, many studies were devoted to *n*-butane isomerization using SZ and related catalysts; this reaction is of special interest due to

* Corresponding author. Fax: +1 303 530 0264.
E-mail address: dfraenkel@eltronresearch.com (D. Fraenkel).
[1] Present address: Chemistry and Biochemistry Dept., Arizona State University, Tempe, AZ, USA.

0021-9517/$ - see front matter © 2010 Elsevier Inc. All rights reserved.
doi:10.1016/j.jcat.2010.06.002

its great commercial importance in fuel processing. In parallel, considerable work was directed toward acidity characterization; especially, many studies involved spectroscopic investigation into probe molecules adsorbed on SZ. Most of those studies concluded that SZ is *not* a superacid even though it may rank as a strong acid similar to common H-zeolites. Thus, the group of Kazansky [6] used diffuse reflectance IR spectrometry of benzene-adsorbed SZ and concluded that SZ is a stronger acid than silica gel but "*weaker than HX zeolite*". (Note that "HX" is a non-crystalline, collapsed FAU structure hence is not a "zeolite" but an amorphous silica-alumina!) Sachtler's and van Santen's groups [7] probed the acidity of SZ by CO and acetonitrile and inferred the acidity strength based on FTIR and NMR measurements, respectively. They concluded that the acid strength of SZ is similar to that of HY but weaker than that of HZSM-5. The exact same conclusion was made by Drago and Kob [8] based on a calorimetry – pyridine adsorption ("cal-ad") technique. Interestingly, the latter authors also showed their SZ sample to effectively isomerize *n*-pentane at room temperature in the liquid phase under batch conditions, but no information was given by them on a parallel reaction with HY or HZSM-5. Calorimetric studies of ammonia-neutralized SZ, yielding heat of adsorption, were conducted by Dumesic and coworkers [9]; they also concluded that the acid strength of SZ is "*not unusually high*" but rather is similar to that of common strong solid acids, e.g., HY.

Earlier, in 1990, Umansky and Hall [10] argued that adsorption studies are inadequate for probing acid strength. This is because (a) strong bases (pyridine, ammonia and the like) do not equilibrate with the various acid sites at ordinary temperatures, (b) when solvent is used, concentration is solvent dependent, (c) chemisorbed bases may decompose on strong acid catalytic sites thereby not "probing" them, and (d) adsorption occurs on both Lewis and Brønsted sites; and thus, proton-generating Brønsted functions cannot be distinguished from just electron-deficient Lewis acid centers. What is even worse is that, as Umansky and Hall noted, "*each time an NH_4^+ or Na^+ neutralizes an effectively covalent Brønsted site, the acidity (intensive factor) of the remaining sites is reduced by charging up the lattice*". These authors thus concluded that "*the only meaningful measure* [of acidity in solids] *must involve the use of a probe in such* [a] *high dilution that the measurement does not perturb the system*". It is, of course, doubtful whether any spectroscopic measurement of adsorbed probe molecule, as mentioned earlier, may satisfy the requirement of a dilution at which the measurement does not perturb the system.

Thus, the overwhelming consensus, based on probe molecule adsorption studies, that SZ is not a superacid did not, in fact, address appropriately the key question asked by Umansky and Hall [10]: "*If we had a solid superacid, how would we recognize it?*" Hall's group, in attempt to answer this question, resorted to isobutane conversion [11], a reaction previously employed by McVicker et al. [12] to distinguish between strong and weak acid solids. The latter authors were the first to draw attention to the virtues of isobutane as reactant that could probe acid strength; they pointed out that based on the fact that C_3 and C_4 carbenium ions formed from this reactant cannot undergo β-scission, product distribution can be greatly simplified compared to that of other paraffinic reactants. McVicker et al. performed a gas-phase isobutane conversion in the range 1–50% conversion to total product, in a differential fixed-bed flow microreactor, at a flow rate (F/W) of 3.47×10^{-5} mol/g s (moles of isobutane flowed per gram catalyst per second). Hall's group, at a flow of 1.12×10^{-5} mol/g s (i.e., three times smaller), conducted the same experiment but at very low conversion, <1%. They measured the temperature at which 1/2% conversion to total product ($T_{1/2\%}$) is achieved and the Arrhenius apparent activation energy close to $T_{1/2\%}$ (E_a). They then attempted to correlate $T_{1/2\%}$ with H_0 as measured by a special spectrophotometric method they devised and employed earlier [10].

While not reporting isobutane conversion testing (i.e., $T_{1/2\%}$ and E_a data) for SZ, Umansky et al. claimed [11] that, based on their diffuse reflectance spectroscopic measurements, SZ is not a strong superacid but rather a solid system approximating the acid strength of sulfuric acid with $H_0 = -12$ (hence they coded it "ZrO_2/H_2SO_4"), "*as might have been anticipated.*" Thus, Hall's group joined the other research groups claiming the same based on spectroscopic-adsorption investigations. Moreover, in 1996, Fărcaşiu et al. [13] boldly contested the notion (and convention) of using H_0 as a criterion for acidity strength in solids (see below), claiming that unlike in the case of liquids, H_0 in solids has no theoretical meaning, and H_0 values measured by Hammett indicators do not reflect real acid strength; this is because the Hammett kinetic treatment, argued Fărcaşiu et al., is not applicable to surfaces on which acid sites are fixed and localized (i.e., the conjugate acid of the indicator forms on the negative surface a "tight ion pair"). To explain the unusually high catalytic activity of SZ, say in *n*-butane isomerization, those authors proposed a one-electron oxidation mechanism leading to cation radicals. In their conclusions, they echoed Sachtler, van Santen and their coworker who had summed up their observations by stating [7] that "*sulfated zirconia is an active catalyst for n-butane isomerization, a reaction conventionally classified as 'acid-catalyzed'*" and then that an "*extremely active catalyst for an 'acid-catalyzed' reaction need not be an extremely strong acid.*"

In view of the unresolved issue of the real acid strength of SZ, as mentioned earlier (for a recent review, see pp. 27–29 in Ref. [2]), Fraenkel [14] took the effort to use Hall's isobutane test (hereinafter referred to as Hall Acidity Test, or HAT) for SZ. He noticed that Hall's $T_{1/2\%}$–H_0 correlation – in one case presented as a linear relationship [11] – lacks theoretical basis. He attempted a simplified kinetic model that indicated that H_0 should, in fact, correlate linearly with $E_a/T_{1/2\%}$. Fraenkel's final equation can be written, in general, as

$$H_0 = \frac{E_a}{2.3RT_x} - Int_x, \tag{1}$$

where *Int* stands for intercept and *x* symbolizes conversion. Experimental data are required for extracting the numerical value of the intercept. These were conveniently taken from Umansky et al. [11], at $x = 0.005$ (1/2%), to yield $Int_x = Int_{1/2\%} = 23.4$ for $T_x = T_{1/2\%}$. Based on this, Eq. (1) yielded for SZ H_0 of about −17.5. Arata et al. later reported a method of estimating H_0 in strong solid acids by argon-TPD and found the H_0 of SZ to be −19 [15]. Their respective H_0 values for H-zeolites, based on visual color change of Hammett indicators, appear some 1–2 unit lower than other literature data (e.g., as in Ref. [11]).

In this paper, we report on an extension of the HAT to a series of strong solid acids varying in acidity strength, which includes SZ. This work was perceived necessary because earlier studies were performed either with the zeolite solid acids, or with SZ, but never *with both systems alongside each other*, in one series. There has been some concern that the test might be sensitive to technical factors relating to the details of the reactor, the experimental procedure and/or the particular catalyst samples used. In the study we report here, which has been briefly presented recently [16], we employed four solid acids: SZ and the three zeolites HM (MOR), HZSM-5 (MFI) and HY (FAU), all at typical elemental compositions and physicochemical characteristics. One objective of this study was to verify that results for the zeolites are in good agreement with those of Umansky et al. [11], and that, examined under almost identical experimental testing conditions, SZ indeed gives the behavior as reported by Fraenkel [14]. Furthermore, by comparing product distributions at ~1/2% conversion, we hoped to be able to draw more specific conclusions on the variation of the isobutane conversion mechanism as a function of acid strength. Moreover,

an attempt is provided here to estimate H_0 values for the catalysts of McVicker et al. [12], and for an HY studied by Hall et al. [17], by extrapolating Arrhenius plots based on >1% isobutane conversions, to 1/2% conversion. Finally, an analogy is drawn between HAT and the conversion of a protonated weak base (ketone) in *liquid* superacids, to grant more credence to the idea that the acidity ranking of solids can be based on the activation energy of the protonation step of a weak base, using Eq. (1). A conclusion is drawn on the interplay of various mechanisms in isobutane conversion, as a function of acidity and its strength, and a novel hydrocarbon conversion pathway, believed suitable for superacids, is proposed.

2. Theoretical background

2.1. Comparability of acidity tests

The work presented here is based on the comparison between acid solid catalysts as obtained by two acidity tests. Specifically, we employed the well-known Hammett indicator test (visual color change), and the chemical reactivity test as measured by isobutane conversion (HAT). The two methods are parallel in being based on the intrinsic tendency of the acid to protonate a very weak, uncharged base, which is the definition of the Hammett-acidity function, H_0. The first method measures H_0 rather directly, whereas the second is an indirect method by which the kinetics of the conversion of the base to products, through chemical transformation, assuming that base protonation is rate determining, is translated to H_0. Also, Hammett indicators give a color change when their pK_a matches H_0, whereas the isobutane test (and for that matter, any weak base conversion test, e.g., another alkane transformation) is based on a single "indicator" (here isobutane) with a single pK_a that does not have to be known; the distinction between solid acids of different strength is done by the different temperatures at which those acids, in a flow microreactor, catalyze a certain low conversion of the base (say, 1/2%) and by the corresponding Arrhenius apparent activation energies at and near this conversion point. Of course, this is valid only as long as the catalytic reaction mechanism can be considered as solely involving Brønsted acid borne carbocations and their chemical/structural transitions. It is somewhat ironic that the isobutane conversion test of acidity was developed (by Hall's group [10,11]) because of a concern that the Hammett indicator method may not be applicable for solid acids. However, the isobutane test turns to be just an indirect way (see below) of estimating H_0! As such, its success is subject to our very ability to measure H_0 by Hammett indicators, for calibration (and comparison). We end up where we started: If the Hammett acidity test is inappropriate for solid acids, so is the isobutane test (or any other test based on an alkane transformation reaction).

Hammett acidity measurements using indicators was done extensively in the literature; within the current study, it was only performed to a limited extent. We wanted to distinguish between at least a few catalysts based on this test, in order to compare their acidity with their catalytic performance. It was thus important to apply the indicator visual test to the specific solid acid samples of the present study. Also, this test was expected to complement and be in accord with the isobutane test (HAT). We next elaborate on the theoretical basis of the Hammett indicator test as used for solids (2.2) and of the isobutane conversion test (2.3).

2.2. Acidity test I: Hammett indicators and their applicability for solid acids

The acidity measurement using structurally related weak base indicators was proposed first in 1932 in the landmark article on acidity functions by Hammett and Deyrup [18]. It was meant for liquid acids, but in 1950, Walling suggested [19] that it could be applicable to solids. Benesi later devised a standard method for applying indicators in the case of solid acid catalysts [20], but presented the method for relatively weak acidities. Following Benesi, other researchers, including those studying very strong superacid solids such as SZ [3,4], used the indicator method in their investigations while applying weaker bases with pK_a of less than −12 [1]. More comprehensive reviews of the method were given in the literature [2,21]; and here, we shall only briefly mention its fundamentals for the sake of further discussing its validity limits for solids.

For a base B reacting with a Brønsted acid, hereinafter referred to, for simplicity, as H^+, according to

$$B + H^+ \Longleftrightarrow BH^+, \tag{2}$$

the transformation of B to BH^+, causing a color change, say from colorless (B) to yellow (BH^+), occurs through a concentration "switchover" during which we pass a point of $[BH^+]/[B] = 1$. At this point, the pK_{BH^+} (pK_a) becomes identical with Hammett-acidity function, H_0 which is defined [18] as

$$H_0 \equiv -\log\left(a_{H^+}\frac{f_B}{f_{BH^+}}\right) = pK_{BH^+} - \log\frac{[BH^+]}{[B]}. \tag{3}$$

Using indicators, it is assumed that the activity coefficient ratio of the base to protonated base, f_B/f_{BH^+} is the same or almost so for different, but structurally related, bases and therefore the acidity function is independent of the particular base indicator used to measure it. A series of indicators with different pK_{BH^+} values is used, and going from the stronger to weaker base, we follow the color change until the color does not change. The acidity is then between the pK_{BH^+} of the last base that gave a color change and the pK_{BH^+} of the first base that did not. For example, we may report an acid as having $-11.35 < H_0 < -8.2$.

There are a few problems relating to extending this test from homogeneous liquid acid media to solid surfaces. First, a color change with a liquid acid is visually more pronounced as it occurs in the liquid phase and not limited to the surface of a solid. Second, usually, solids have less acid concentration than liquid acids, as the acid is a function residing on the solid surface, whereas in liquid acid it is "neat". For example, 100% sulfuric acid is 100% acid (H^+ function) while sulfated zirconia has typically only ~5%wt sulfate over 95% "unseen" zirconia; "luckily", all the sulfate sites are exposed, i.e., none are incorporated inside the ZrO_2 bulk. A color change of 5% acid on a surface of a support is more difficult to follow than a color change of a liquid acid at 20 times higher concentration. Third, in many solid acids, there is acid strength inhomogeneity owing to the solid structure being heterogeneous (e.g., in amorphous silica-alumina, solid phosphoric acid). As a result, we measure only a portion of the acidity each time. However, we may assume that in many cases, especially in highly crystalline solids, where the surface is well-defined structurally and chemically, most acid sites are either of about the same type and similar strength, or fractioned into groups of (almost) same-strength sites; this at least seems to be the case with high-silica zeolite molecular sieves, in their H-form (see Ref. [10] and references therein) and in crystalline sulfated metal oxides, such as (tetragonal) sulfated zirconia. Fourth, and related to the above, acid sites on surfaces are influenced by their neighbors and as acid–base neutralization proceeds, next-neighbor sites are weakened or eliminated (see above); this problem, which does not occur in liquid acids (where acid species are assumed totally independent of one another), causes alteration of the acid strength of a site. We therefore may assume that if some small portion of the acid sites gave a color change, since they are of a proper strength for protonating an indicator base, then

their next-neighbors may become weaker by this very base protonation and therefore unable to protonate the same base. Thus, an inherent (false?) assumption in measuring acid strength of solid surfaces is that *acid sites are independent of other acid sites*; this requirement is sometimes hard to swallow. Hammett indicators are added in such a dilute solution that the assumption is that only a small portion of the acid protonates the indicator base; this, of course, further reduces the intensity of the color used to distinguish between B and BH^+ on solid surfaces. Fifth, to complicate things even more, Hammett bases are aromatic compounds that, whether protonated or not, adsorb strongly on solid surfaces thus sometimes causing coloration and/or blockage of the surface Brønsted acid functions. Sixth, we have to assume not only that the surface is homogeneous in terms of acid site distribution and strength, but also that the surface behaves as a strong electrolyte [20], which could be considered as two-dimensional [20] or a fractal between 2D and 3D. As such, we have to treat the solid acid surface as a homogeneous acid *solution*, even though the acid sites are not freely moving as in liquid acids. As a possible response to Fărcaşiu's argument [13] (see above), one may propose that even though acid centers are fixed on a surface, the *protons are free to move* (i.e., rapidly exchange between different acid centers) in what may be regarded as a "two-dimensional acid solution" over the solid surface. Seventh – and most important in very strong solid acids – a lack of sufficient acid quantity, when we are limited to solid surfaces, causes more vulnerability of the acid sites to impurities, such as ubiquitous humidity, than in the case of liquid acids of very high strength. Even worse, with Lewis acids (such as SO_3/ZrO_2) that become Brønsted acids upon addition of H_2O (e.g., in SZ), the adequate amount of moisture required for strongest acidity may be confusing: We may either not add enough H_2O to create sufficient number of Brønsted sites, or we may add too much H_2O, thus weakening the acidity of those sites after their creation, through "titration" by H_2O molecules acting as base. This concern was first raised by Fraenkel [22] in regard to the special transient activity of SZ in alcohol conversion and its dependence on acid strength.

With so much restriction and uncertainties regarding the theoretical basis and application of the H_0 measurement, how can we rely on this method? The answer is that we simply look for consistencies and straightforward correlations; if H_0 measurements are in agreement whether we choose the indicator method or the isobutane conversion method or any other acidity measurement (see below), and if further, this agreement is supported by a coherent mechanistic behavior in the catalytic process that logically follows acid strength changes (as we shall try to show later), then we can apparently trust the obtained H_0 values at least on a semi-theoretical level by which acids – liquid and solid – can be distinguished based on strength (as defined) and the consequent chemical reactivity.

2.3. Acidity test II: isobutane 1/2% conversion

It is very well known and clearly documented [23] that in acid-catalyzed reactions, the logarithm of the rate constant correlates, usually linearly, with H_0. This goes back to the original paper of Hammett and Deyrup [18] that offered this basic kinetic relation, for first-order reactions, without a basic kinetic development; such a development was later given [23] for various reaction mechanisms. The issue of the current study is not to ignore and repeat the literature but to extend the above kinetic correlation to *activation parameters*; specifically, to derive, in a step-by-step manner, a plausible correlation between H_0 and the Arrhenius apparent activation energy, E_a. Furthermore, this derivation is geared toward providing a convenient tool for kinetically interpreting isobutane 1/2% conversion data of various solid acids, as in HAT. More specifically, our aim is to be able to correlate the isobutane conversion kinetics, as a function of temperature, with H_0.

2.3.1. Rate equation expressed in terms of H_0

In a Brønsted acid-catalyzed reaction of a weak base B, we assume that Eq. (2) (i) is rate determining, (ii) follows a *pseudo* first-order kinetics, (iii) occurs with very small conversion of B, x (i.e., $x \ll 1$), (iv) involves a very small fraction of the catalytic (Brønsted) sites, and, (v) has a reaction rate $Rate = k_{ef}[B]$, where k_{ef} is proportional to the "degree of protonation" [2,18], $[BH^+]/[B]$. Therefore,

$$k_{ef} = k' \frac{[BH^+]}{[B]}. \tag{4}$$

Since $[B]$ remains virtually unchanged, we can set $k'' = k'/[B]$, so $k_{ef} = k''[BH^+]$. From Eq. (4),

$$\log k_{ef} = \log k' + \log \frac{[BH^+]}{[B]}, \tag{5}$$

and Eq. (3) can be substituted into (5). But to do so, we need to factorize the activity coefficient ratio in Eq. (3) when applied to our weak base (say, B is isobutane), to have B correlated properly with the structurally related Hammett bases (indicators), for which we assume that the f-ratio behaves similarly. Therefore, for our $[BH^+]/[B]$ ratio,

$$H_0 = pK_{BH^+} - \log \frac{[BH^+]}{[B]} - \log F_c, \tag{6}$$

F_c being a constant factor, specific to the reactant base we choose. Substituting Eq. (6) into (5) gives

$$\log k_{ef} = \log k' + pK_{BH^+} - H_0 - \log F_c, \tag{7}$$

or

$$k_{ef} = \frac{k'}{F_c \times K_{BH^+}} e^{-2.3H_0}. \tag{8}$$

Replacing the pre-exponential factor in Eq. (8) by k, gives

$$k_{ef} = k e^{-2.3H_0}. \tag{9}$$

Eq. (9) is, as expected, identical with the equation $H_0 + \log k = \text{constant}$, proposed by Hammett and Deyrup [18] for the relation between the acidity function H_0 and the rate of an acid-catalyzed reaction (see above); Hammett's "k" is the current k_{ef}, and "constant" is the current $\log k$. Based on Eq. (9), the overall rate equation is

$$Rate = k e^{-2.3H_0}[B]. \tag{10}$$

2.3.2. Temperature effect

To account for the effect of temperature (T), we assume that, compared to the Arrhenius effect, the change of H_0 with T is small and, to a first approximation, negligible. We thus ignore temperature effects on $f_B f_{H^+}/f_{BH^+}$, or otherwise, resort to the relation between H_0 and f_{H^+}, at constant H^+ concentration and about constant f_B/f_{BH^+} (see Section 5.1), i.e.,

$$-\log f_{H^+} \approx H_0 + Const. \tag{11}$$

Due to its crucial role in the development of the kinetic correlation between isobutane conversion and H_0, this point needs some elaboration as done in Appendix A. In view of the above assumption (supported by the discussion in Appendix A), H_0 will be treated here as if it is not temperature dependent and we shall argue that while this postulate is kinetically not entirely satisfactory, it leads – as will be shown below – to an effective and believable correlation between H_0 and the kinetics of isobutane conversion.

For k_{ef} we, therefore, set

$$k_{ef} = k_{efo}e^{-\varepsilon}, \tag{12}$$

ε being the dimensionless Arrhenius factor E_a/RT. Likewise,

$$k = k_o e^{-\varepsilon_o}, \tag{13}$$

and combining Eqs. (13), (12), and (9),

$$k_{efo}e^{-\varepsilon} = k_o e^{-(\varepsilon_o + 2.3H_0)}. \tag{14}$$

ε_o is $(E_a/RT)_o$ corresponding to $H_0 = 0$. k depends on the temperature but, to a first approximation (see above), not on acidity; therefore, its pre-exponential factor, k_o is a "universal" kinetic parameter, independent of both T and H_0. When comparing different solid acid catalysts under gas-phase continuous-flow conditions, at a constant reaction rate, we may assume that this constant rate is translatable to T_x – the temperature giving constant low conversion fraction x, i.e., $x \ll 1$. We may set

$$Rate = k_{ef}[B] = x(F/W) = k_{efx} = Constant, \tag{15}$$

F being the reactant gas flow rate, W the catalyst mass (and we assume a constant density of active acid sites, see below), and k_{efx} the rate at temperature T_x. We thus get, according to Eq. (12),

$$k_{efox} = k_{efx}e^{\varepsilon_x}, \tag{16}$$

where ε_x is E_a/RT_x, and based on Eqs. (12) and (14),

$$k_{ox} = k_{efx}e^{(\varepsilon_{ox} + 2.3H_0)}. \tag{17}$$

k_{efx} is consistent only with Eqs. (16) and (17) being identical, and thus, $k_{efox} = k_{ox}$ (=non-constant for constant k_{efx}), and

$$\varepsilon_x = \varepsilon_{ox} + 2.3H_0. \tag{18}$$

2.3.3. Practical expressions

If k_{efx} is given (say, 1/2% constant conversion) and ε_x is measured from Arrhenius plots and T_x, then ε_{ox} can be calculated from Eq. (18), and k_{efox} (=k_{ox}) from Eq. (16) (or (17)). When ε_x is plotted against H_0, it should yield a straight line with slope 2.3 (=ln 10) and intercept ε_{ox}. At different k_{efx} values (different x's), a family of parallel straight lines would be obtained. It is convenient to write Eq. (18) as Eq. (1) where Int_x equals $(E_a/2.3RT_x)_o$ (corresponding to $H_0 = 0$). For $T_x = T_{1/2\%}$, $Int_x = Int_{1/2\%}$ was estimated [14], based on Hall's work [11], to be 23.4 (see below, Section 2.3.4). Thus, HAT should respond to the approximate kinetic expression

$$H_0 = \frac{E_a}{2.3RT_{1/2\%}} - 23.4. \tag{19}$$

For the interconversion between H_0 and $\varepsilon_{1/2\%}$ as acidity scales, see Appendix B.

The kinetic development of This Work demonstrates that $T_{1/2\%}$ is not the only important factor in determining the acidity of the catalyst using HAT; another factor, which is seemingly more important, is the Arrhenius apparent activation energy, E_a measured near $T_{1/2\%}$. The kinetic factor that correlates with H_0 was found to be $E_a/RT_{1/2\%}$ ($\equiv\varepsilon_{1/2\%}$). $Int_{1/2\%} = 23.4$ is the semi-theoretical "limit of superacidity" in HAT, as $-H_0$, because we cannot allow negative values for E_a; obviously, this "limit" is only pertaining to the isobutane test. In other words, no lower value than −23.4 can be measured in HAT for H_0. This means that HAT cannot distinguish between acids stronger than −23 on the H_0 scale. Interestingly, Sommer and Jost [24] found the superacid with "highest acidity" to be HF-(90%molar)SbF_5 with $-H_0 = 23$–24. However, at such a low H_0 value, acidity cannot be measured but only estimated. (For more on this, see below).

2.3.4. Agreement of Eq. (19) with Hall's results

The results of Hall's group [11] were reexamined based on the kinetic expression correlating H_0 with the isobutane reaction parameters; for this, the $E_a/T_{1/2\%}$ values of Hall's various solid acids were calculated and placed on a $-H_0$ vs. $E_a/T_{1/2\%}$ presentation, Fig. 1. The solid straight line with the forced $-1/2.3R$ slope represents Eq. (19). By least-square regression, this line is placed such that $Int_{1/2\%} = 23.4$. The two broken lines are the upper and lower limits of accuracy if one assumes ±1 accuracy in H_0, i.e., that $Int_{1/2\%}$ is 23.4 ± 1. In this case, all experimental points for the zeolites (HM, HY and H-beta) fall within the straight line accuracy region. However, the values for the silica-alumina samples (M-46 and N-631-L) [11] are clearly outside the correlation range. As we shall claim later, this is due to the too high reaction temperature needed for 1/2% conversion with these weak acids, causing a mechanistic change that bypasses the Brønsted acid mechanism; new pathways create an alternate, more facile route to products, thereby reducing the activation energy. If H_0 of the silica-alumina solid acids is about −6 [11], then based on Fig. 1, one should expect E_a to be ~65 kcal/mol (typical to thermal reactions [25]); instead, the experimentally derived value was only 40–50 kcal/mol [11].

3. Materials and methods

3.1. Gases and liquids

Helium gas (99.995%, zero-grade purity) and air (zero-grade purity) were purchased from General Air and used without further purification. The 10%vol isobutane in helium from General Air (prepared by Matheson Tri-Gas) had 10.01% isobutane with ±2% accuracy, and the balance was 99.999% He. The isobutane in the gas mixture was found by gas chromatography (see below) to contain <0.003%wt propane and <0.001%wt normal butane as the only detectable impurities. *n*-Pentane (⩾99.0%, HPLC grade) was purchased from Aldrich (Cat. # 34956) and used without further purification. It was found, by GC analysis, to contain 0.23% isopentane.

3.2. Characterization instruments

The solid acids of this study were characterized by powder-XRD over a Philips x-ray powder diffractometer using Cu-$K\alpha_1$ radiation (λ = 1.5405 Å), cryogenic N_2 physisorption using Quantachrome Quadrasorb SI and NOVA 2000e instruments, thermogravimetric analysis using Shimadzu TGA-50 instrument, scanning electron microscopy (SEM) using a JEOL JSM-5610 instrument, with gold sputter coat (20 s) applied to the examined sample, and transmis-

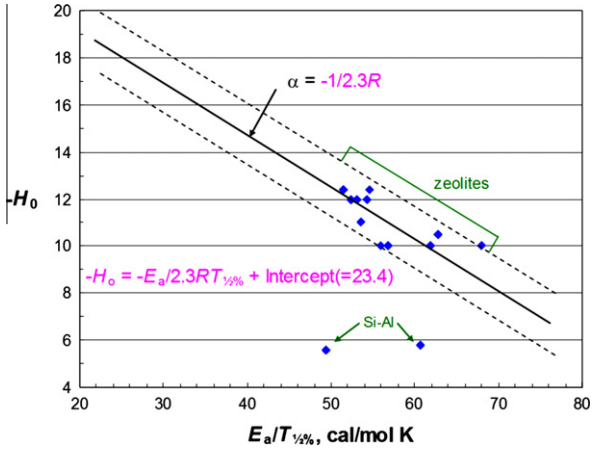

Fig. 1. $-H_0$ vs. $E_a/T_{1/2\%}$ analysis for Hall's data (Ref. [11]).

sion electron microscopy (TEM) using a Philips CM10 instrument with 100 kV accelerating voltage; powder suspensions were applied to a holey carbon 300-mesh grid and dried under a heat lamp before being analyzed.

3.3. Solid acids

Two types of solid acids were used in this study, sulfated tetragonal zirconia (SZ) and molecular sieve zeolites; the zeolites were HZSM-5 (MFI), nanocrystalline large-port mordenite (MOR), coded *nc*-HM and a Linde Y faujasite (FAU) HY. The latter zeolite was purchased from Aldrich, as NH_4Y, and was calcined to form the acidic HY. The NH_4Y zeolite as obtained had, by elemental analysis, approximately 65% (by weight) SiO_2, 22% Al_2O_3 and 2.5% Na_2O hence was 90% ion-exchanged with NH_4^+; in the calcined H-form, this translates to 72.6% SiO_2, 24.6% Al_2O_3 and 2.8% Na_2O. The Si/Al atom ratio (SAR) was 2.51. After calcination at 500 °C for 3 h, the zeolite had a BET surface area of 626 and a *t*-plot area of 210 m^2/g; the total pore volume was 0.265 cm^3/g. The other zeolites were prepared by proprietary methods in our laboratory. The HZSM-5 had SAR = 36, BET surface area of 405 and *t*-plot area of 120 m^2/g; its XRD spectrum was that of a pure, high-quality MFI structure. The *nc*-HM, with 90.7% SiO_2 and 9.3% Al_2O_3 (by EDX), hence SAR = 8.3, had ~50 nm average crystallite size as calculated by the Scherrer equation (using Philips X'pert software package); instrument line broadening compensation was done with the XRD Si line at ~28° 2θ. The same average size was observed in TEM micrograms. The surface area (m^2/g) was 373 (BET) and 96 (*t*-plot). A standard large-port mordenite (average crystal size ~200 nm) from Tosoh, Japan, given as gift by Matheson Tri-Gas (Longmont, Colorado), was used for calibrating the *nc*-HM. In both cases, XRD spectra were those of a pure MOR structure. A dealuminated version of *nc*-HM, Deal-*nc*-HM, with average crystal size (Scherrer) of 38 nm, BET SA of 419 and *t*-plot area 151 m^2/g, was obtained by digesting *nc*-HM in 85% HNO_3 at 100 °C for 1 h, followed by calcination at 500 °C for 3 h. SZ was prepared according to a literature recipe [26]; after calcination at 600 °C, it had a pure tetragonal ZrO_2 structure, 1.65%wt sulfur and a BET (equal to *t*-plot) surface area of *ca.* 100 m^2/g. The average crystallite size was calculated (Scherrer equation, see above) as well as found by TEM to be <10 nm. A typical TEM micrograph of SZ is shown in Fig. 2; aggregates of tiny, ~3-nm crystallites are clearly observed with a very uniform physical habit.

Hammett acidity measurements by the indicator method were done according to the standard method of Benesi [20,21].

3.4. Reactions

3.4.1. Gas-phase isobutane conversion

Gas-phase conversion of isobutane was performed using a continuous-flow, differential microreactor as described previously [14,26]. Run conditions and product analyses were kept close to those of the original Hall's work [11] (one difference, considered insignificant, was the use of He instead of N_2 as carrier gas and as diluent for isobutane). Specifically, 400 mg catalyst was placed in the ¼″ stainless steel upright tubular reactor. The catalyst powder was formed into 150–250 μm granules by pressing, grinding and sieving between 60- and 100-mesh screens. The catalyst sample was freshly activated *in situ* at 520 °C for 1 h, prior to the activity test, under a gas mixture flow of 200 cm^3/min air and 100 cm^3/min He, regulated each by a calibrated Aalborg rotameter. The catalyst was then purged with pure He for 15 min. The reactor was set to the target temperature meant to achieve close to 0.5% isobutane conversion. When the target temperature was reached, the helium gas was replaced by the isobutane–helium mixture (see above); the latter gas mixture, prior to reaching the reactor, was passed over an activated mordenite (HM) trap; the gas flow rate was 60 cm^3/min controlled by a 5850E mass flow controller from Brooks Instruments. An analysis of the effluent gas was performed 10 min later. The gas chromatographic analysis, over a Shimadzu GC-17A instrument, with an FID detector, and equipped with a Supelco Petrocol DH capillary column, lasted usually for about 30 min. If conversion was below target, the temperature was raised; if conversion was above target, the temperature was lowered. A usual set of runs at different temperatures around 1/2% conversion and the subsequent GC analyses lasted for about 5 h. There was no substantial detected effect of time-on-stream on catalyst performance during that period.

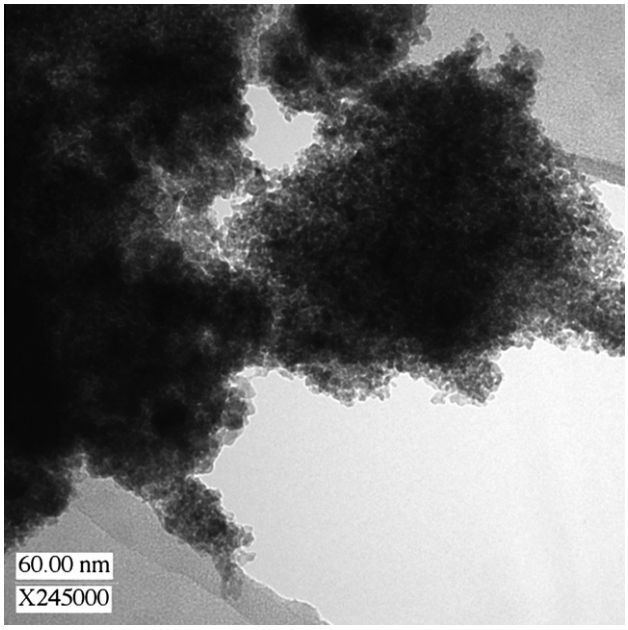

Fig. 2. TEM micrograph of SZ.

3.4.2. Liquid-phase n-pentane conversion

The conversion of *n*-pentane in the liquid phase was performed according to a method used and briefly reported before [27]. A 0.4-g catalyst sample, in powder form, was placed in a vial, activated at elevated temperature, then cooled and quickly transferred to a desiccator and allowed to cool there to ambient temperature. Then, using a crimper, the vial was sealed with an aluminum-lined rubber septum. Through the septum, 1 ml of *n*-pentane liquid (see above) was injected. The mixture was shaken occasionally during a period of tens of hours. Samples for GC and GCMS analysis were taken periodically with a syringe, through the septum. The GC analysis was performed over a Shimadzu GC-17A gas chromatograph equipped with a Supelco Petrocol DH capillary column (as above) and by GCMS analysis over Shimadzu GC-17A/QP-5000 instrument, equipped with Alltech AT-1 capillary column.

4. Results

4.1. "Hall Acidity Test" (HAT)

4.1.1. Isobutane conversion vs. temperature

The four solid acids used in this study, i.e., HY, HZSM-5, HM and SZ, showed activity in the gas-phase conversion of isobutane, which extended over a broad temperature range, from about 100 to 450 °C. The pattern of isobutane conversion near 1/2% for the four acids, as percent conversion vs. temperature, is shown in Fig. 3. The corresponding Arrhenius plots are presented in Fig. 4.

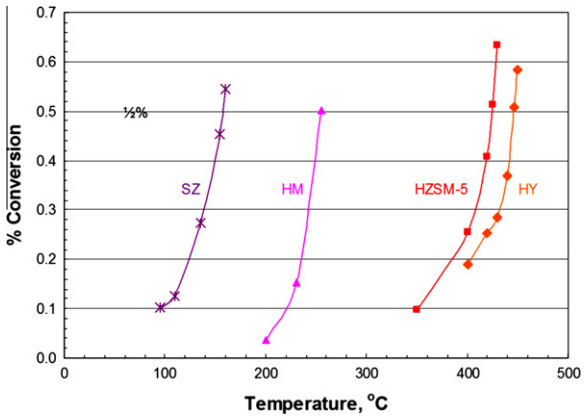

Fig. 3. Isobutane conversion near 1/2% as a function of temperature.

By interpolation of the straight lines obtained and from their slopes, $T_{1/2\%}$ and E_a were extracted, respectively. The $E_a/T_{1/2\%}$ values were placed on the $-H_0$ vs. $E_a/T_{1/2\%}$ correlation line to obtain the corresponding H_0's. This is demonstrated in Fig. 5. Results of the various HAT parameters are given in Table 1; they are also compared with similar parameters from Hall's work [11]. Our HY gave $H_0 = -9$ which is in agreement with the -10 value obtained by Hall's group (e.g., as in Table 1) for a number of HY samples. Our HM sample gave H_0 of -13.8 that is somewhat lower than Hall's values (-12.4), but not in conflict with those data [11]. HZSM-5 gave $H_0 = -10$; Hall's group did not report *measured* H_0 values for HZSM-5 samples for which they performed the isobutane test; however, calculated H_0 for HZSM-5 (Table 1), based on Hall's data and employing Eq. (19), is close to our values (some of Hall's ZSM-5 samples gave lower calculated values, ~ -13). Our results for the zeolites seem to generally agree with Hall's in terms of both the nominal H_0 values and the acid strength ranking; this is in spite of understandable differences between the actual zeolite samples used in the two studies. Thus, HAT appears reasonably reproducible for the zeolite acids. Furthermore, a repeat of our work a year later with the same samples we used before (Table 1), but over a different microreactor system, has shown reasonably good agreement with our previous results, with somewhat lower H_0 value for HM. The repeated work gave the same acid strength ranking of the four solid acids studied, as before.

Compared to the zeolites, SZ stands out in the HAT in providing a very low H_0, -18.5 (Fig. 5). This corroborates Fraenkel's result [14] (-17.5) and is also close to the more recent estimate of Arata et al. [15] based on Ar-TPD (-19) in addition to supporting the old estimate of Hino and Arata [3] (<-16). In the second set of tests with the same four acids (see above), the SZ results were similar (Table 1, "repeat").

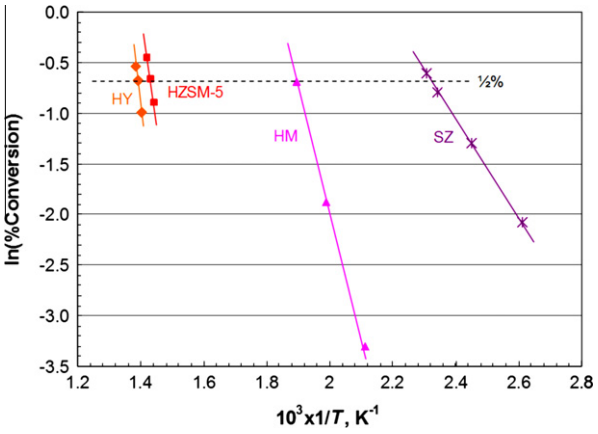

Fig. 4. Arrhenius plots based on Fig. 3.

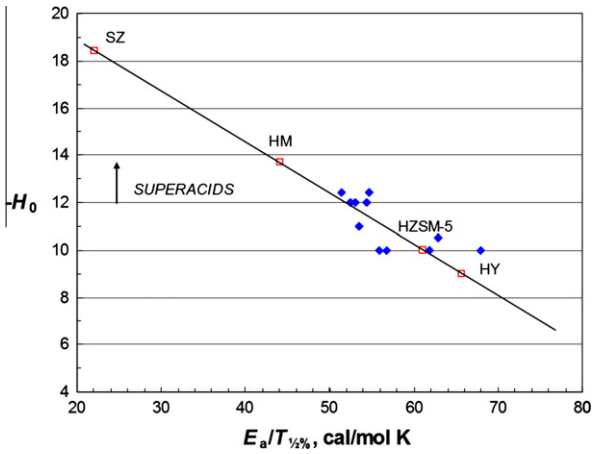

Fig. 5. $-H_0$ vs. $E_a/T_{1/2\%}$ line as in Fig. 1, with Hall's results (closed symbols); $E_a/RT_{1/2\%}$ results of This Work (open symbols) are placed on the line to estimate H_0.

Table 1
HAT parameters.

Catalyst	$T_{1/2\%}$ (°C)	E_a (kcal/mol)	$\varepsilon_{1/2\%}$	$-H_0$
SZ	157.5	9.54	11.2	18.5
HM	256.0	23.4	22.3	13.7
HZSM-5	424.6	42.7	30.9	10.0
HY	446.3	47.3	33.2	9.0
Repeat				
SZ	153.5	7.85	9.3	19.3
HM	258.8	18.4	17.5	15.8
HZSM-5	415.0	43.1	31.6	9.6
HY	428.0	43.6	31.4	9.7
Hall's[a]				
HM	221	25.4	25.8	12.2
HZSM-5	400	37.8	28.1	11.2
HY	406	42.0	30.8	10

[a] Based on Ref. [11]; HM – LZ-M8, HZSM-5 – "HZSM-5(35)", HY – "H-Y(8.1)". $T_{1/2\%}$ and E_a are as published; $\varepsilon_{1/2}$ and $-H_0$ calculated according to the present treatment.

4.1.2. Product distribution

Fig. 6 compares chromatograms of the four solid acid catalysts of this study as obtained near 1/2% conversion. As expected based on the literature [11,12], product distribution is considerably different for the various acids and drastically different between the extremes represented by SZ and HY. For each acid, the product distribution (Table 2, as %wt) is about constant at different conversions around 1/2%; this is demonstrated for HM and HY in Fig. 7 (as %mol). It is very clear that with SZ, the reaction pattern is composed of two pathways – butane isomerization and isobutane disproportionation; even some isohexane is observed, obviously as the product of a secondary transmethylation reaction between (protonated) isopentane and isobutane. On the other extreme of HY, the product is mostly C_2–C_4 paraffins and olefins that can be produced by dehydrogenation and cracking reactions of *n*-butane (isomerization product) and isopentane (major disproportionation product). HM and HZSM-5 seem to give intermediate product distribution patterns, between the two extremes; HM leans toward SZ, and HZSM-5 toward HY. The hydrocarbon product distribution for HM, as given in Fig. 7a, shows that, as stoichiometry requires for disproportionation, the molar ratio of propane-to-isopentane

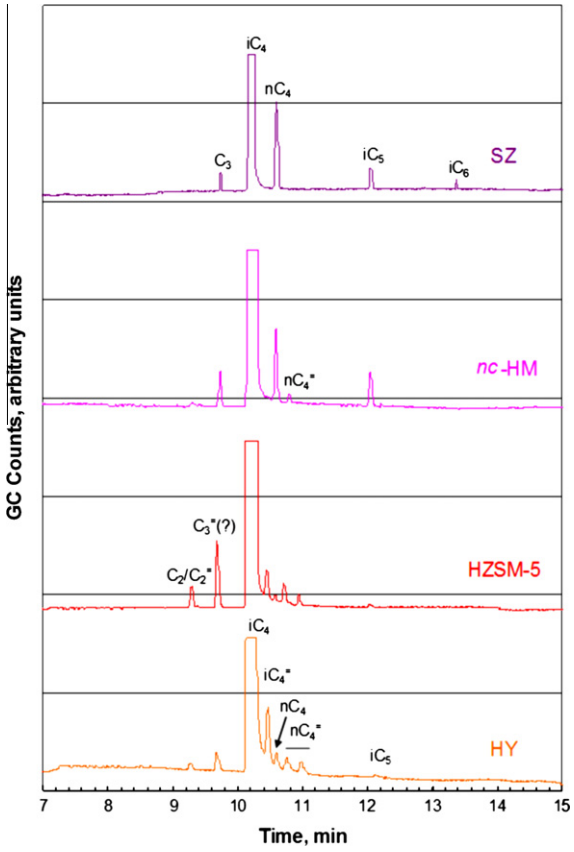

Fig. 6. Typical gas chromatograms near 1/2% isobutane conversion.

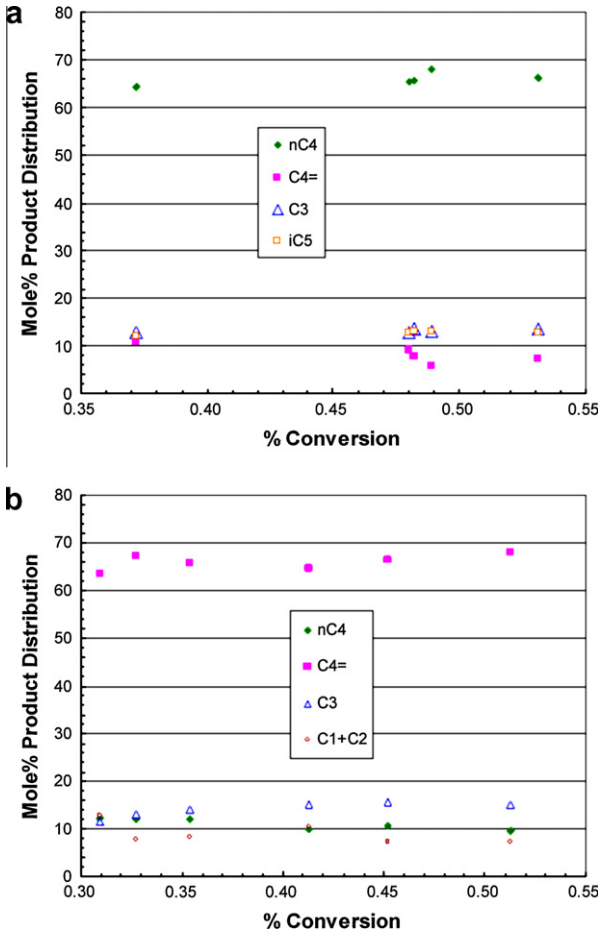

Fig. 7. Hydrocarbon product distribution in isobutane conversion as a function of percent conversion near 1/2%. (a) HM, (b) HY.

Table 2
Hydrocarbon product distribution at about 1/2% isobutane conversion.

C-Prod. (%wt)	SZ	*nc*-HM	HZSM-5	HY
C_1–C_2	–	trace	10.4	3.1
C_3	9.4	20.4	32.2	10.6
$iC_4^=$	–	–	26.3	49.3
nC_4	77.4	49.9	8.6	15.5
$\Sigma nC_4^=$	–	6.8	20.4	21.6
iC_5	13.2	22.8	2.1	trace
Total	100.0	99.9	100.0	100.1

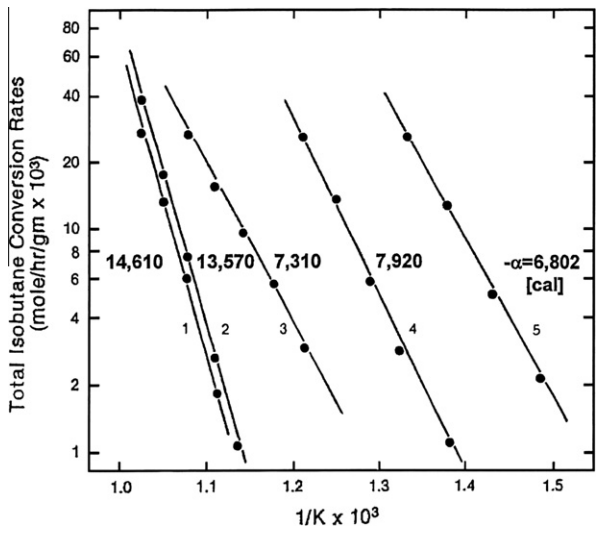

Fig. 8. McVicker's isobutane conversion data (Ref. [12]): Arrhenius plots and their respective (recalculated) slopes. Single-digit numbers next to lines refer to various cases (blank and catalysts), see text and Table 3.

is approximately unity; this indicates that neither isopentane nor propane is produced by a route other than isobutane disproportionation. In this particular case (HM), about 65% of the converted isobutane was isomerized, 25% disproportionated and ~10% dehydrogenated. The very different molar product distribution of HY (Fig. 7b) features the C_4 olefins (total) as over two-third of the entire product and *n*-butane concentration is low, ~10%. Note that the results presented in Fig. 7 are based on the "repeat" work (see also Table 1), whereas the results of Table 2 are those of the first testing series. The overall agreement between Fig. 7 and Table 2 is good, with HM showing somewhat lower *n*-butane and higher C_3 values; this, if not reflecting an analysis artifact, is apparently because some C_3 may have been produced in this case by cracking. Table 2 also indicates a maximum C_3 in HZSM-5 with almost no net iC_5 produced (i.e., almost all the C_3 results from cracking). Bizreh and Gates [28] reported that HZSM-5 (SAR = 70), at similar temperature (429 °C) and conversion (0.37%), but under pulse microreactor conditions, gave 5.8%wt CH_4, 0.77% C_2H_4, 18.8% C_3H_6, 65.7% C_4H_8 and 8.9% C_5H_{10}; they did not detect C_3H_8, C_4H_{10} and C_5H_{12} in the product mixture. In HY, there is much smaller concentration of C_3 while isobutene concentration doubles compared to the HZSM-5 case (Table 2). The latter product is not detected over the superacids SZ and HM. Higher isomerization than disproportionation in SZ compared to HM indicates that the

former reaction may be more strongly affected by the acidity; this could imply that the reaction pathways leading to isomerization and disproportionation may be inherently different (such as monomolecular vs. bimolecular, respectively [29], see Section 5).

In summary, from the foregoing it is obvious that with a series of solid catalysts of varying acid strength, not only is *activity* in isobutane conversion influenced, as reflected by $T_{1/2\%}$ and E_a of HAT, but also *selectivity*; this implies changes in the mechanism of the isobutane conversion process. This issue will be further addressed in Section 5.

4.1.3. Analysis of literature isobutane conversion data by extrapolation to 1/2% conversion

McVicker et al. [12] studied comparative isobutane conversion by conducting a set of five experiments with catalysts having acid strength that varied from none to weak to strong: 1 – blank (mullite beads), 2 – $MgAl_2O_4$ (non-acid), 3 – amorphous silica-alumina, 4 – F-Al_2O_3, and 5 – HY (LZ-Y82). Their results were presented as Arrhenius plots; in Fig. 8, we have added to those plots the numerical values of the slope (α) as recalculated by us to improve accuracy of the E_a calculation. The McVicker work was done with conversion levels between about 1 and 50%. Extrapolation of the Arrhenius lines to 1/2% conversion [corresponding to 0.000625 mole isobutane converted per (g cat × h)] provided $T_{1/2\%}$. We tried to estimate H_0 for the above five cases based on Eq. (19). The results of this analysis are summarized in Table 3. A difficulty encountered in doing this was that the F/W value of McVicker was three times larger than that of the HAT (see above and Table 3). In evaluating H_0, we could ignore the higher space velocity assuming that its influence is small – it is expected to increase $T_{1/2\%}$ compared to that of the HAT only by about 10–20 °C and therefore not significantly affect $E_a/T_{1/2\%}$. However, a quantitative estimate of the space velocity effect can be done based on the theoretical $E_a/T_{1/2\%}$–H_0 correlation developed above. Assume k_{efx} for a certain F/W (say, the HAT's – 1.12×10^{-5} mole g^{-1} s^{-1}). For a different space velocity, $(F/W)'$, we have k'_{efx}. From Eq. (15), $k'_{efx} = k_{efx} \times (F/W)'/(F/W)$. Since $k'_{ox} = k_{ox}$, it follows from Eq. (17) that

$$\varepsilon'_{ox} = \varepsilon_{ox} - \ln\frac{(F/W)'}{F/W}. \tag{20}$$

For correcting H_0 values for the space velocity effect in Cases 1–5 (McVicker's), we thus have to use, as intercept of Eq. (1), $Int'_{1/2\%} = 22.9$ (instead of 23.4, the value of $Int_{1/2\%}$).

Along with McVicker's results, we added in Table 3 "Case 6" based on a study by Hall et al. [17] with the same HY (LZ-Y82); here, we used a similar analysis, but Hall's work employed a different space velocity; again a H_0 correction can be applied (Table 3) using Eq. (20). In Table 3, E_a values in parentheses are those given by McVicker et al. [12] and they are seen to be somewhat different than the recalculated values. The Table is divided into two groups: The left-hand side group is that of Cases 1–3 that involve very high reaction temperatures, with $T_{1/2\%} > 450$ °C, and Case 4 for which $T_{1/2\%} < 450$ °C but the experiments were performed at temperatures above 450 °C. The other group, on the right-hand side, includes the HY zeolite Case 5 and Hall's Case 6 (with the catalyst of Case 5); also, for comparison, HAT results of Umansky et al. [11] are provided in the last column, using the same solid acid. This right-hand side group is characterized by relatively low reaction temperatures and by $T_{1/2\%} < 450$ °C. The first-group members with $T_{1/2\%} > 450$ °C are believed to represent a non-acid, thermal-radical mechanistic regime (Cases 1 and 2) and a mixed catalytic mechanism due to mostly Lewis (not Brønsted) acid regime combined with a thermal-radical regime [12] (Case 3). Case 4 is a borderline between Cases 3 and 5, where, at higher temperatures, the mechanism was mostly radical-like [12] and at the lowest run temperatures, the mechanism was a mixture of radical and acid (perhaps Brønsted) types. Case 4 employs a catalyst (F-Al_2O_3) that appears to be a very strong Brønsted acid, almost as strong as 100% sulfuric acid, but the result of the analysis is offset toward lower H_0 (higher acidity) because even at 1% conversion (lowest point), the temperature is still higher than 450 °C. Indeed, product analysis in this case (at high conversion) shows mostly radical mechanism derived alkane/alkene distribution [12]. In reality, F-Al_2O_3 could be a weaker acid with say, $H_0 = -10$ or so, but still much stronger than silica-alumina (Case 3). The H_0 values estimated for the first group, given in parentheses, are considered false and meaningless as they are based on too small E_a values due to the facilitation of the isobutane conversion by free radicals and/or carbenium ions created by Lewis acid hydride abstraction (see Section 5).

The second group (Table 3, right-hand side) is believed to represent an almost 100% Brønsted acid regime. H_0 values appear very reasonable. Case 5 employs an Arrhenius line based on two points below and two points above 450 °C; all points fit nicely with the straight line (Fig. 8), and the slope and extrapolation to half-percent conversion look more reliable than in Case 4. The corrected

Table 3
HAT analysis of isobutane conversion data above 1% ("Simulated HAT").

Mechanism	Thermal-radical, Lewis acid				Brønsted acid		
Catalyst	Blank	$MgAl_2O_4$	SiO_2–Al_2O_3	0.9% F-Al_2O_3	LZ-Y82 (FAU, HY)		
Case	1	2	3	4	5	6[a]	HAT[b]
F/W [c]	3.47	3.47	3.47	3.47	3.47	1.524	1.12
Lowest T[d] (°C)	627	612	553	452	402	380	
$T_{1/2\%}$ (°C)	602.6	592.8	491.5	434.7	366.8	368.9	349
$T_{1/2\%}$ (K)	875.6	865.8	764.5	707.7	639.8	641.9	622
$-\alpha$ (in kcal)	14.61	13.57	7.31	7.92	6.80	7.73	
E_a[e]	67.2[f]	62.4	33.6	36.4	31.3	35.2	32.6
(E_a[g])	(59)	(62)	(33)	(39)	(35)		
$\varepsilon_{1/2\%}$/ln 10	16.8	15.8	9.64	11.28	10.73	12.04	11.4
$-H_0$[h]	(6.7)[i]	(7.6)[i]	(13.8)[i]	(12.2)[i]	12.8	11.4	12.0
$-H_0$, corr'd[j]				(11.6)[i]	12.2	11.2	

[a] Ref. [17].
[b] Analysis based on data from Ref. [11].
[c] Mole g^{-1} s^{-1} × 10^5.
[d] Lowest temperature at which isobutane conversion was run.
[e] kcal/mol; recalculated from Arrhenius plot.
[f] Typical to thermal decomposition; e.g., see Ref. [25].
[g] kcal/mol; from Ref. [12].
[h] Calculated from Eq. (18).
[i] Wrong value, see text.
[j] Corrected for space velocity, see text.

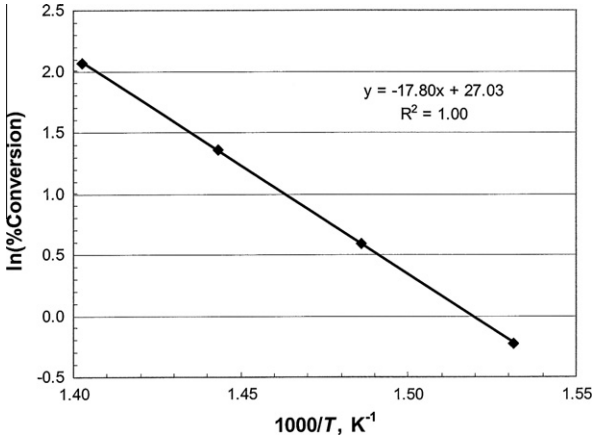

Fig. 9. Hall's isobutane conversion data (Case 6 in Table 3): An Arrhenius plot for LZ-Y82 based on Ref. [17].

H_0 value, −12.2, agrees with the HAT value for the same solid acid (last column, Table 3). There is also a very good agreement with the other HAT parameters. Hall's Case 6, with the same acid, was studied at 1–8% conversion. The Arrhenius analysis gives a perfect straight line (Fig. 9) indicating that the kinetics developed above is applicable to higher (perhaps an order of magnitude higher) conversions than ~1/2%. Case 6, however, provides somewhat higher than expected E_a, thus, about a unit larger H_0. Overall, LZ-Y82 appears as strong as 100% H_2SO_4.

Hall's results [11] with silica-alumina (e.g., $T_{1/2\%}$ = 518 °C, E_a = 39.1 kcal/mol for N-631-L) do not contradict with McVicker's (Table 3), and in another report [30] of Hall's group, the silica-alumina M-46 gave at 460 °C a product distribution reflecting pure radical mechanism [12] (see Section 5) with only H_2, CH_4, $C_3^=$ and $iC_4^=$ detected, and with the required interrelation $[H_2]/[iC_4^=] \approx [CH_4]/[C_3^=] \approx 1$. In view of this and the foregoing analysis and discussion, it is entirely justified to omit the silica-alumina HAT data in the kinetic analysis as presented above (Fig. 1).

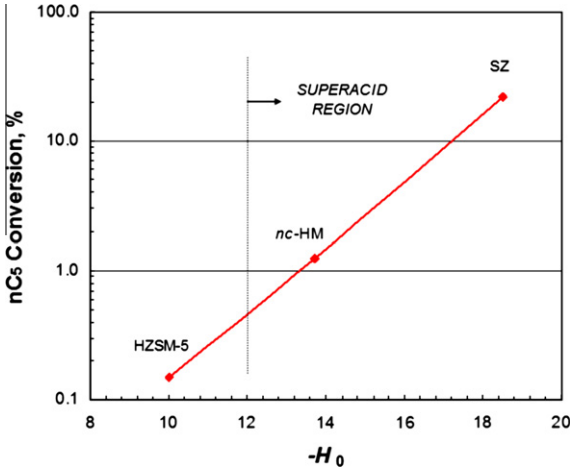

Fig. 10. *n*-Pentane conversion as a function of H_0.

4.2. Other acidity probes

4.2.1. n-Pentane conversion

It appears that superacidity can be probed by *n*-pentane conversion, as illustrated in Scheme 1, when the reaction is conducted at room temperature in the liquid phase, under batch conditions. Both Magic Acid® and HCl–$AlCl_3$ are known to catalyze this reaction; they are both strong superacids [2,29,31]. In the reaction, *n*-pentane isomerizes to isopentane that subsequently disproportionates to equal molar parts of isobutane and isohexane (various isomers). At high conversion, there is extensive secondary and tertiary disproportionation, eventually resulting in a whole range of mostly isoalkane mixture of iC_4–iC_9. The fact that SZ also catalyzes this *n*-pentane conversion, and in the very same manner, suggests that SZ has acid strength that is comparable to those of the above acids, thus being a strong superacid. This is supported by the fact that, in contrast, 100% H_2SO_4 (H_0, −12) and weaker acids such as H-zeolites and silica-alumina are incapable of converting *n*-pentane at ambient conditions (Scheme 1).

As a further illustration of the compatibility of the *n*-pentane conversion test with the isobutane test, Fig. 10 depicts final nC_5 percent conversion data vs. $-H_0$ based on HAT for the HZSM-5, HM and SZ of this study. The acidity ranking is shown to follow the extent of *n*-pentane conversion (and *vice versa*) with HZSM-5 being entirely inactive, HM showing marginal activity and SZ exhibiting considerable activity (conversion) under similar reaction conditions. With SZ, the mixture, after 2 days, contained 48% (by weight) isopentane and 52% disproportionation products at about equal molar proportions of isobutane and isohexane + isoheptane. We may infer that, as a general rule, *n*-pentane is converted to isoalkanes at ambient conditions in the liquid phase under batch reaction conditions only over superacids. This is fully consistent with the fact that *m*-ZrO_2 (monoclinic zirconia, see below), like HZSM-5, was totally inactive in pentane conversion. H_2SO_4(95%) ($-H_0$, ~9) gave 1.1% conversion suspected as being due mainly to a redox reaction because of the detection of an SO_2 peak in GCMS analysis. This oxidation may have produced pentanol. Under comparative reaction conditions, an H_2SO_4/*m*-ZrO_2 combined catalyst gave similar results as those of the liquid acid, whereas a H_2SO_4/SZ combination yielded 7.8% pentane conversion to a mixture similar in composition to that of pure SZ (at 21% conversion).

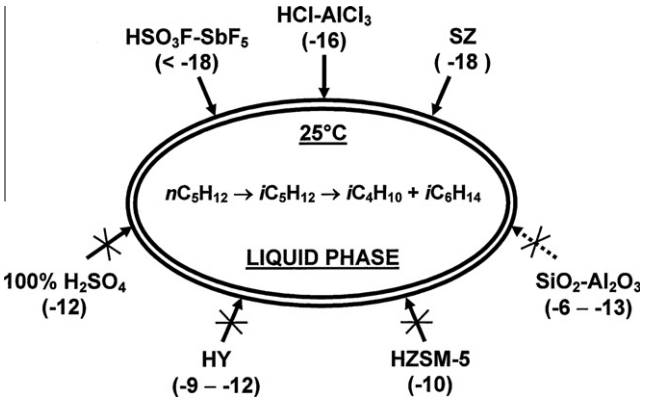

Scheme 1. Conversion of *n*-pentane at ambient conditions: activity of different acids and its dependence on H_0 (given in parentheses). Crossed arrows symbolize lack of catalytic activity, crossed broken arrow denotes expected lack of activity.

4.2.2. Hammett indicators

Umansky and Hall [10], in applying their special spectrophotometric method, reported their results in what they called the "bracketed method", i.e., the range of pK_a between the weakest indicator base that could be protonated and the next weaker one that could not. They presented the range $-13.7 < H_0 < -12.4$ for the HM samples, and $-12.4 < H_0 < -8.7$ for HY samples [11]. We have employed the Benesi technique [20] for the specific solid acids of the present study. HY and HZSM-5 could not be tested because of their coloration in benzene. Typical data are shown in Table 4 where + signs designate color change (from colorless to yellow), − signs represent lack of coloration, and +/− signs indicate a weak, but clearly evident, color change. H_2SO_4(95%) was used as a reference and it gave the expected range of H_0, as in the literature [1,21]. Also, as expected, a monoclinic (*m*-) zirconia did not color even the strongest base of the series, anthraquinone, because that solid is a non-acid. In contrast, SZ colored all bases. The test was repeated for SZ a few more times, at different periods separated by months, and results were fully reproducible. We have also found that coloration on SZ was particularly intense after this solid acid was freshly activated at 450 °C; this is perhaps due to the retaining of optimal amount of moisture for highest acidity under such conditions, over the SZ. The test for SZ fully confirms the results of Hino and Arata [3]. HM samples exhibited H_0 values higher than those of the HAT, but gave nevertheless the correct acid strength order, being as strong or stronger than H_2SO_4(95%) and weaker than SZ. The result for dealuminated HM is closer to the HAT result.

Table 4
Acid strength measurement by Hammett indicators.[a]

pK_{BH^+}	−8.2[b]	−11.35[c]	−12.44[d]	−13.16[e]	−14.52[f]	−16.04[g]	H_0 range
m-ZrO_2	–	–	–	–	–		>−8.2
H_2SO_4(95%)	+	–	–	–	–		−11.4 to −8.2
nc-HM	+	–	–	–	–		−11.4 to −8.2
Deal-*nc*-HM	+	+/–	–	–	–		−12.4 to −11.4
SZ	+	+	+	+	+/–	+/–	<−16.0

[a] Color change marked + and no change marked –; +/– indicates weak or marginal color change and is regarded as positive change.
[b] Anthraquinone.
[c] 4-Nitrotoluene.
[d] 1-Fluoro-4-nitrobenzene.
[e] 1-Chloro-3-nitrobenzene.
[f] 1-Fluoro-2,4-dinitrobenzene.
[g] 1,3,5-Trinitrobenzene.

4.2.3. Strong base adsorption on acid sites: What does adsorption of ammonia and amines on solid acids really probe?

4.2.3.1. Gas-phase proton affinity vs. proton transfer in solution, over solid acids. Gorte's group [32,33], through calorimetric studies of ammonia and amine adsorption in acid zeolites, attempted to find out whether a straightforward (e.g., linear) correlation exists in solid acids between gas-phase proton affinity (PA) and solution-phase proton transfer in water ($-\Delta H^{o}_{prot,S}$), for various amines. They concluded that whereas the (differential) heat of adsorption (ΔH_{ads}) correlates effectively with PA, its correlation with $-\Delta H^{o}_{prot,S}$ is poor. Two problems with this conclusion immediately emerge: 1. The "correlation" (Fig. 4 in Ref. [32], ΔH_{ads} vs. PA) and "non-correlation" (Fig. 5, ΔH_{ads} vs. $-\Delta H^{o}_{prot,S}$) presentations are on different size scales and thus create false visual impression. 2. The comparison was done with alkyl amines of different groups (primary, secondary, tertiary). The above researchers used data from the work of Aue et al. In one report [34], Aue et al. demonstrated that PA of amines correlates linearly with $-\Delta H^{o}_{prot,S}$. However, the correlation was only within the *same* group of amines, *not* between different groups. Obviously, if A correlates with B, and B correlates with C, then A also correlates with C. The results of Aue et al. ("A correlates with B") thus seem at odds with the results of Gorte ("B correlates with C but A does not"). A close examination reveals that whereas Gorte and coworkers used $-\Delta H^{o}_{prot,S}$ values from the above Aue work, they were careful to avoid using the parallel PA data because a few years later, Aue and Bowers published revised PA values for the same alkyl amines [35]. Gorte's group, therefore, compared their ΔH_{ads} data with the $-\Delta H^{o}_{prot,S}$ values of Ref. [34] and with the revised PA values of Ref. [35]. In their later publication [35], Aue and Bowers did not examine the correlation between their revised PA and the $-\Delta H^{o}_{prot,S}$ data. We therefore took the initiative to do this here. Fig. 11 presents plots of revised PA vs. $-\Delta H^{o}_{prot,S}$ for primary, secondary and tertiary amines. The correlation curves, three well-separate straight lines, are similar to those reported by Aue et al. for the unrevised PA data [34]. Again here, it is fully established that values belonging to different amine groups do not correlate. Therefore, attempting to correlate them with ΔH_{ads} is doomed to fail. Fig. 12 shows that, put on a proper scale and based on only primary alkyl amines (and ammonia), ΔH_{ads} *does* correlate, at similar quality, with *both* PA (revised) and $-\Delta H^{o}_{prot,S}$. It is thus obvious that Gorte's conclusion, mentioned above, is false; using it to advocate [32,33] differences between the applicability of gas-phase and liquid (aqueous)-phase reactions on solid acids, such as acid zeolites, is highly misleading. Specifically, Gorte states [32] that "*a gas-phase reference condition is a much sounder starting point for understanding zeolite acidity than any approaches that rely on aqueous* pK_a *values and solvent-filled zeolite pores like Hammett-acidity function correlations.*" However, Gorte's ΔH_{ads} data, and their same correlation with PA and with $-\Delta H^{o}_{prot,S}$ values (Fig. 12), seem to strongly support, if not prove, the opposite.

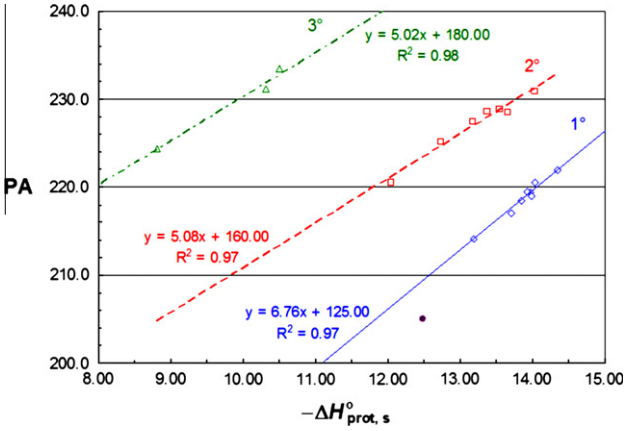

Fig. 11. Correlation between PA and $-\Delta H^{o}_{prot,S}$ (in kcal/mol) for primary, secondary and tertiary amines, based on Refs. [34,35]. The lone purple symbol (at PA = 205) represents ammonia.

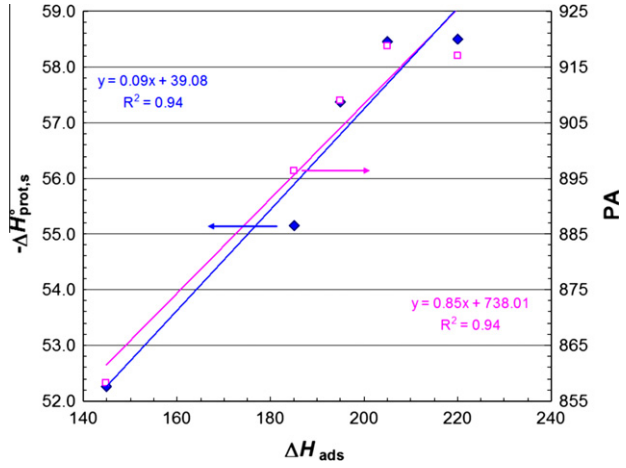

Fig. 12. Correlation between PA (empty squares), $-\Delta H^{0}_{prot,S}$ (full diamonds) and the differential heat of adsorption of ammonia and primary amines, in kJ/mol. PA, $-\Delta H^{0}_{prot,S}$ data are as in Fig. 11, ΔH_{ads} data are from Ref. [32]. Symbols from left to right represent, respectively, ammonia, methylamine, ethylamine, isopropylamine and *n*-butylamine.

4.2.3.2. Density and strength of Brønsted acid sites on solids. In addition to their heat of adsorption studies of ammonia and amines,

Parrillo and Gorte measured, by calorimetry, TGA and TPD methods, the adsorption *capacity* of ammonia and amines in zeolites [36]; they also followed the heat of adsorption as a function of the degree of surface coverage [32,36]. They found that ΔH_{ads} is approximately constant up to a base-to-Al molar ratio of about unity. Since the framework tetrahedral Al content of high-SAR zeolites, in the H-form, is directly related to the number of Brønsted acid sites, Gorte's group concluded that (1) ammonia/amine adsorption probes the number of Brønsted acid sites in high-silica zeolites where sites are considerably far apart from one another, therefore avoiding next-neighbor site–site interaction, and (2) all sites are essentially of the same acid strength. While conclusion (1) is plausible and quite straightforward, we challenge conclusion (2). First, and contrasting with the perception as expressed in the literature (for example, of Dumesic's group [37]), there is no known theoretical basis for the claim that if different acid sites adsorb a base with the same enthalpy change, then the sites should be of the same acid strength. Nor is there any reason to expect that a very strong (or superacid) Brønsted acid site should increase the heat of adsorption compared to a weaker site. A change [37] or a lack of change [32,36] in ΔH_{ads} as a function of the degree of surface coverage may be the results of different factors none of which relating to acid strength of the Brønsted function (oxygen-bound proton).

Gorte's group proposed [32,33] that ΔH_{ads} of the process

$$B(g) + ZOH \rightarrow BH^+ \cdots ZO^-,$$

with B(g) being a base in the gas phase and ZOH representing a zeolite in the acidic, H-form, can be separated to the different steps involved in the overall process with their respective enthalpy change contributions:

(1) $B(g) + ZOH \rightarrow B(g) + H^+ + ZO^-, \quad \Delta H_1$
(2) $B(g) + H^+ + ZO^- \rightarrow BH^+(g) + ZO^-, \quad \Delta H_2$
(3) $BH^+(g) + ZO^- \rightarrow BH^+ \cdots ZO^-, \quad \Delta H_3$

ΔH_1 is the negative of the proton affinity to ZO^-, ΔH_2 is proton affinity to the base B, and ΔH_3 is the BH^+ affinity to ZO^-. Obviously, $\Delta H_{ads} = \Delta H_1 + \Delta H_2 + \Delta H_3 = -(-\Delta H_1) + PA + \Delta H_3$. PA is an intrinsic property of the base and is not affected by the type and strength of the acid. $\Delta H_3 - (-\Delta H_1)$ is a difference between two affinities to ZO^-, that of BH^+ and that of H^+, which tend to cancel each other's effect at any acidity strength, hence remaining about constant. The latter enthalpy change is contrasted by PA. ΔH_1 is a large negative value (meaning that detachment of H^+ from ZOH requires an input of considerable energy). PA (=ΔH_2) is positive but much smaller in absolute value than ΔH_1, and ΔH_3 adds sufficient energy to compensate for the "loss" in ΔH_1. Therefore, ΔH_{ads} is much smaller than PA, but it directly (and linearly) relates to PA (see above discussion and Fig. 12) since $\Delta H_1 + \Delta H_3 \approx$ Constant. Gorte's group recognized this fact. The reason that ΔH_1 and ΔH_3 compensate each other is that the first represents detachment of H^+ from ZO^- and the other, attachment of BH^+ to the same ZO^-. Since within the same group of bases, say primary alkyl amines, the effective BH^+ size is about constant, $\Delta H_1 + \Delta H_3$ should also be about constant. For example, according to SCF calculations in the modeling of ammonia adsorption on H-zeolites [38], $\Delta H_1 \approx -327$ kcal/mol, and $\Delta H_2 \approx 217$ kcal/mol; from microcalorimetry, $\Delta H_{ads} \approx 36$ kcal/mol. This provides $\Delta H_3 \approx 146$ kcal/mol, and we have $\Delta H_1 + \Delta H_3 \approx -181$ kcal/mol; the latter figure is, as expected, very close to the negative of the intercept of the PA vs. ΔH_{ads} line in Fig. 12 (176 kcal/mol) that is an average value for ammonia and the primary alkyl amines. This outcome is very plausible since the affinity of H^+ to ZO^- should be much larger than the affinity of NH_4^+ (a larger cation) to ZO^-. A change in Brønsted acid strength is only a change in the effective size of the conjugate anion base, such as ZO^- (see Section 5). A stronger acid will have larger ZO^- (in general, "A^-") but the net effect on ΔH_1 and on ΔH_3 will be about the same, hence canceled in the sum of these two enthalpies. Therefore, the higher the PA (=ΔH_2), the larger the ΔH_{ads}, and stronger and weaker acid sites will provide about the same enthalpy of base adsorption. The heat of adsorption thus depends mostly on the nature of the base, as indeed shown by Gorte's group [32], and it may be about constant with sites of non-constant acid strength. Acid–base neutralization occurs as long as the acid is strong enough to protonate the base (and ammonia and simple amines are quite strong bases, with pK_{BH^+} of a few positive units; for example, the pK_{BH^+} of NH_3 is 9.26; in comparison, the strongest base used by us as Hammett indicator has pK_{BH^+} of −8.2, hence is 300 quadrillion times a weaker base than ammonia!).

The conclusion from this subsection is that, quite apparently, ammonia and amine adsorption on solid acids is *not* a probe of acidity strength, only of acid site density (i.e., the number of acid sites per unit size of a given solid acid sample).

4.3. Density of strongest Brønsted acid sites on solids

The previous subsection has left us with a puzzle: If, unlike Gorte's claim, the Brønsted acid sites of zeolites are not of the same acid strength, and at least, acid strength cannot be inferred from the heat of adsorption of a base on the solid acid surface, how do we estimate the number of strongest acid sites? This problem is directly related to the present isobutane conversion study since in the HAT we refer to flow and conversion *per gram* of solid acid; this provides "rate of reaction" but not "turnover frequency" (TOF) values. Obviously, we should consider only the strongest Brønsted sites among all sites available, because those sites will dominate the reaction of a very weak base, such as isobutane. In other words, the number of "less-than-strongest" acid sites is irrelevant in this reaction, and so it is in the Hammett acidity test. We may advance by offering a simplified model for zeolites for assessing the amount of strongest sites as percent of all strong H^+ sites, or "% Str. H^+". We shall subsequently offer a plausible estimate of the acid site density in SZ. We shall *a priori* claim that we should be interested only in the *order of magnitude* of the surface Brønsted acid site concentration for the kind of analysis done here.

Hall's group, in addition to measuring $T_{1/2\%}$ and E_a for about 20 solid acids [11], also provided rates of isobutane conversion at 370 °C, a temperature allowing interpolation of kinetic curves characterized by effective Arrhenius behavior. Those rates, as (mole iC_4 converted) g^{-1} s^{-1}, ranged from 6×10^{-11} for silica-alumina with $H_0 = -5.8$ to $\sim 6 \times 10^{-5}$ for HM with $H_0 = -12.4$. Thus, the six orders of magnitude difference in rate of isobutane conversion followed the six unit change in H_0 and in the right direction. The above researchers also provided TOF values at 370 °C based on the estimation of the number of Brønsted acid sites from that of lattice aluminum sites not compensated by residual Na^+ (Na_2O). HY with $H_0 = -10$ gave TOF_{370} of 1.2×10^{-6} s^{-1}, and HM with $H_0 = -12.4$ gave 3.5×10^{-2} s^{-1}. The four orders of magnitude difference in TOF_{370} is, thus, not reflected by the ~2 unit H_0 difference of the strong acids. (However, considering the error in H_0, the "real" difference could indeed be four units, for example, with H_0 being −9 for HY and about −13 for HM, as found in the present study, Table 1.)

It is quite apparent that Hall's TOF values are not adequately reflecting acid strength because they relate to the *entire* number of Brønsted acid sites; in reality, however, only a fraction of the acid sites are "the strongest". In the analysis proposed here, we also "count" sites by the number of non-neutralized lattice Al atoms, but we make a further working assumption that in HY, only one Brønsted site per unit cell (192 T atoms, T = Si + Al) is "the

strongest". Thus, % Str. H^+ is 100 when [T]/[Al] = 192 and SAR = 191. A general expression for this function is % Srt. $H^+ = ([T]/[Al])/1.92$. We further consider only Al that is non-neutralized, or $[Al]_{nn} = [Al] - [Na]$ and therefore,

$$\%\ \text{Str. } H^+ = \frac{[Si] + [Al] - [Na]}{1.92([Al] - [Na])}. \tag{21}$$

This equation is defined within the approximate limits of $[Al]/[Na] \geqslant 5$ and $[Si]/([Al] - [Na]) \geqslant 2.8$. For HZSM-5, it looks appropriate to consider that one acid site per unit cell (T = 96) would constitute "100% strongest sites" but we may flexibly assume, without losing essence, that only one site per *two* unit cells is "strongest" and constitutes "100%" of all sites, in order to place HZSM-5 on the same scale as that of HY. In this case, HZSM-5 with one framework Al (and one OH) per unit cell, or 96 T atoms, i.e., with SAR = 95, represents a "% Str. H^+" of 50. Eq. (21) can thus be extended to HZSM-5, and we arbitrarily extend it further to any other H-zeolite, e.g., HM. Table 5 presents calculation of the estimated gram-equivalent of strongest H^+ per gram solid acid for the various zeolite samples for which HAT was employed. Presented are Hall's samples along with the samples of This Work. Eq. (21) is used to estimate % Str. H^+ and the values obtained in each case are used to estimate the number of g-equiv. H^+/g. As seen, in all cases, the acid site concentration is about constant; on average, 0.88×10^{-4}. % Str. H^+ varies between ~2 (for sample 10) and 23 (sample 11). We thus assume that practically, zeolite acids have up to one-fourth of their entire acid sites being the "strongest"; the majority of the Brønsted acid sites, strong as they may be, remain "less-than-strongest" and therefore, practically not participating in the reaction with the weakest base that can be protonated. In the case of the isobutane reaction, this means that the effective sites are only a small fraction of all Brønsted sites.

The case of SZ is obviously different than that of the zeolites. Here, we take the liberty of assuming that *all* Brønsted sites are of equal acid strength. The problem is that there is seemingly no clue as to how many sites reside on the SZ surface. Our SZ sample is a typical one (many such samples are reported in the literature in regard to alkane conversion catalysis), with 1.65%wt S content and thus, 5.2×10^{-4} g-equiv. S per gram. There can only be a rough estimate of the S/H^+ atomic ratio of SZ in the activated state. Fraenkel, based on alcohol conversion studies over SZ, suggested [22] that, to be superacidic, SZ has to have a S/H_2O ratio (corresponding to S/H^+) between about 4 and 70. Xu and Sachtler [39] estimated the S/H^+ ratio to be 12.5 (for 1.0%wt S and calcination at 650 °C), whereas Mastikhin et al., base on ^1H NMR data, estimated for a sample calcined at 600 °C, a range of values of 8–16 [40]. If SZ is visualized as a polysulfuric acid supported on zirconia, then for $H_2S_2O_7$ ($S/H^+ = 2$) the known H_0 is −14.4 [1], whereas for $H_2S_3O_{10}$ ($S/H^+ = 3$) H_0 is ~−14.9 [1]. We choose for the current analysis an intermediate S/H^+ value of 6 (noting that as long as this value is within an order of magnitude from the true value, our analysis is "safe"). This places the site density (per g) of Brønsted units on SZ very close to the value of the zeolites, i.e., $5.2 \times 10^{-4}/6 = 0.87 \times 10^{-4}$ g-equiv. H^+ per gram solid acid. [We should note, in passing, the interesting finding of Dumesic and coworkers [41] that SZ, to which 0.75×10^{-4} moles of H_2O per gram (corresponding to 0.75×10^{-4} g-equiv. H^+ per gram) was added, had a maximum catalytic activity in *n*-butane conversion; however, it is unknown how much moisture (hence H^+) was in the sample initially.]

According to the above analysis, we assume that the *surface* concentration of strongest acid sites on the SZ is 3–4 times higher than in the zeolites: $\sim 9 \times 10^{-7}$ g-equiv. H^+ per m^2 vs. $\sim 2.5 \times 10^{-7}$. For SZ, this means an average area of 1.85 nm^2 per Brønsted acid site and an average site–site distance of about 1.35 nm. In the zeolite case, the parallel values are 6.67 nm^2 and 2.6 nm. The above surface values seem plausible: In SZ, the average S–S distance (i.e., distance between adjacent sulfate groups) is 0.56 nm, and if about six S groups are present per one H^+ site, an H^+–H^+ distance that is double the S–S distance appears very reasonable. In ZSM-5, a distance of 2.6 nm corresponds to acid OH sites ("H^+") being placed, on average, two unit cells apart (*c*-parameter, 13.142 Å). In faujasite (Y), with the cell parameters being $a = b = c =$ 24.345 Å, that distance approximately agrees with sites residing one unit cell apart.

Table 5
Estimate of the density of strongest Brønsted acid sites in zeolites.

Solid acid	Source[a]	Composition, (mol/g) × 100				SAR	% Str. H^+	(g-equiv. Str. H^+)
		SiO_2	Al_2O_3	Na_2O	H^+ (by diff.)			per g × 10^4
HY	3	1.2867	0.2039	0.0323	0.3433	3.15	2.47	0.85
	4	1.3067	0.2069	0.0073	0.3992	3.16	2.23	0.89
	5	1.3133	0.2078	0.0003	0.4150	3.16	2.17	0.90
	6	1.5033	0.0912	0.0048	0.1727	8.24	5.06	0.87
	7	1.4000	0.1559	0.0016	0.3085	4.49	2.88	0.89
	8	1.4483	0.1245	0.0074	0.2342	5.82	3.74	0.88
	9	1.4550	0.1245	0.0016	0.2458	5.84	3.60	0.89
	10	1.2617	0.2363	0.0074	0.4577	2.67	1.96	0.90
	This Work	1.2100	0.2412	0.0452	0.3920	2.51	2.13	0.83
HZSM-5	11	1.6317	0.0206	0.0016	0.0380	39.63	22.91	0.87
	12	1.6267	0.0235	0.0002	0.0467	34.57	18.65	0.87
	13	1.6250	0.0245	0.0016	0.0458	33.15	19.00	0.87
	14	1.6083	0.0343	0.0016	0.0654	23.44	13.33	0.87
	15	1.5567	0.0637	0.0016	0.1242	12.21	7.05	0.88
	16	1.5667	0.0588	0.0016	0.1144	13.32	7.65	0.88
	This Work	1.6280	0.0225	0.0000	0.0450	36.18	19.36	0.87
HM	17	1.4217	0.1431	0.0016	0.2830	4.97	3.14	0.89
	18	1.4950	0.1000	0.0016	0.1968	7.48	4.48	0.88
	19	1.5350	0.0765	0.0016	0.1497	10.04	5.86	0.88
	20	1.5150	0.0892	0.0016	0.1752	8.49	5.02	0.88
	This Work	1.5120	0.0912	0.0000	0.1824	8.29	4.84	0.88
"H-Zeo"	Limit	1.6593	0.0043	0.0000	0.0087	191.00	100.00	0.87
								Ave: 0.88

[a] Numbers represent samples as reported in Ref. [11].

If we accept the above estimation of acid site concentration in the solid acids of the current work, then we also accept the idea that "rate of reaction" for SZ and H-zeolites is parallel to TOF, with a proportionality factor of $\sim 0.9 \times 10^{-4}$. In the HAT, the flow (F/W) is 1.12×10^{-5} moles (of iC_4 flowed) per g per s, and therefore, at 1/2% conversion, 5.6×10^{-8} isobutane molecules have been converted per g per s. Thus, the $TOF_{1/2\%}$ value is $\sim 6.2 \times 10^{-4}\ s^{-1}$. In HAT, the various solid acids are distinguished from one another, in terms of acid strength, not by $TOF_{1/2\%}$ but by the temperature at which this isobutane conversion rate is attained, i.e., $T_{1/2\%}$.

Some clarification seems necessary in regard to the $TOF_{1/2\%}$ value. This value may look quite small: only 2.2 molecules are converted per H^+ site per hour. However, not only is a small fraction of the isobutane converted, but also a very small fraction of the (strongest) acid sites are employed in the catalysis. This is apparent from Eq. (2) that is shifted strongly to the left. We recall that, unlike ammonia and amines, isobutane does not neutralize the acid but rather leaves it mostly intact. For example, if the equilibrium constant of Eq. (2) is $10^{-4}/B$, then the actual $TOF_{1/2\%}$ is $\sim 6\ s^{-1}$ or so. At 1/2% conversion, this is a quite high turnover number. Finally, even though we believe that the acid site concentration analysis proposed in this subsection is very reasonable, we nevertheless are fully aware that it is highly speculative; it, thus, serves only as an initial site density estimate meant to rationalize our HAT results and put them in due perspective with respect to the literature on strong solid acid catalysts in alkane transformation.

4.4. Correlation between acid strength and the activated complex obtained by weak base protonation

The HAT kinetic analysis assumes that $k = k_o \times \exp(-E_a/RT)$, i.e., follows Arrhenius' relation. At 1/2% conversion, $k_{1/2\%} = k_o \times \exp(-E_a/RT_{1/2\%})$. With $k_{1/2\%}$ estimated as $\sim 6.2 \times 10^{-4}\ s^{-1}$ (see above), k_o can be calculated and correlated with E_a. As could be expected, a compensation behavior [42] is observed with good linearity between $\ln k_o$ and E_a. This is shown in Fig. 13 for the catalysts of Table 1 and Fraenkel's SZ [14]. The straight line has an intercept zero and a slope of 0.5557, hence the isokinetic temperature, T_{iso} is 909 K. We can further assume that the theory of absolute rates (transition state theory) can be applied here to estimate thermodynamic activation parameters. With $k_o^o = k_B T/h \approx 10^{13}\ s^{-1}$ (k_B, Boltzmann's factor; h, Plank's constant), $\Delta G^{\ddagger}$ and $\Delta S^{\ddagger}$ of the transition state (or activated complex) in the rate-determining step can be extracted if $E_a \approx \Delta H^{\ddagger}$. We have

$$k = k_o^o \exp\left(\frac{-\Delta G^{\ddagger}}{RT}\right), \tag{22}$$

and therefore,

$$k_{1/2\%} = k_o^o \exp\left(\frac{-\Delta G^{\ddagger}}{RT_{1/2\%}}\right) \approx k_o \exp\left(\frac{-E_a}{RT_{1/2\%}}\right). \tag{23}$$

Since $\Delta G^{\ddagger} = \Delta H^{\ddagger} - T\Delta S^{\ddagger}$,

$$k_o \approx k_o^o \exp\left(\frac{\Delta S^{\ddagger}}{R}\right). \tag{24}$$

Thus, $\ln k_o \approx 0.5051 \Delta S^{\ddagger} + 29.934$. Obviously, with decrease in $\ln k_o$, $\Delta S^{\ddagger}$ becomes more negative implying higher order in the transition state complex. In HAT, we propose that the rate-limiting step is isobutane protonation. The isobutonium complex that electrically compensates for the negatively charged site (conjugate base) on the surface, and apparently associates to a great extent with this anionic entity, is more ordered compared to the ground state of free isobutane and a protonic surface site. An increase in acidity means a higher effective anionic size (see above, and in Section 5) with more electron delocalization, which tends to destabilize the $H^+ \cdots A^-$ state more than the $H{-}iC_4^+ \cdots A^-$ state, the stronger the acid, the larger the effect. Therefore, overall, a higher disorder in the ground state coupled with higher order in the transition state causes $\Delta S^{\ddagger}$ to be negative even for medium-strong acids (e.g., HY) and *highly* negative for very strong acids (e.g., SZ). This analysis contrasts with that of Xu and Sachtler [39], based on Brouwer [43], according to which the transition state is a protonated alkane without contact (hence physical, chemical and structural relation) with the negative counterpart ionic entity. Brouwer developed his model for liquid superacids, but even in the liquid state, at high acid concentration, much of the acid is apparently in the associated state and not in the ionized, fully dissociated state. In this regard, the liquid state and solid state of protonic acids may bear similar properties. The above researchers further associated the activation parameters with the transition between carbenium ions of different branching levels. They assumed that $\Delta G^{\ddagger} \approx \Delta H^{\ddagger}$ since $\Delta S^{\ddagger}$ (likened to that in the gas phase) is very small so its contribution is negligible. While such an assumption is plausible in the gas phase, it is not so in the paired state of a carbocation and a negative center (conjugate base), whether in the liquid or solid phase.

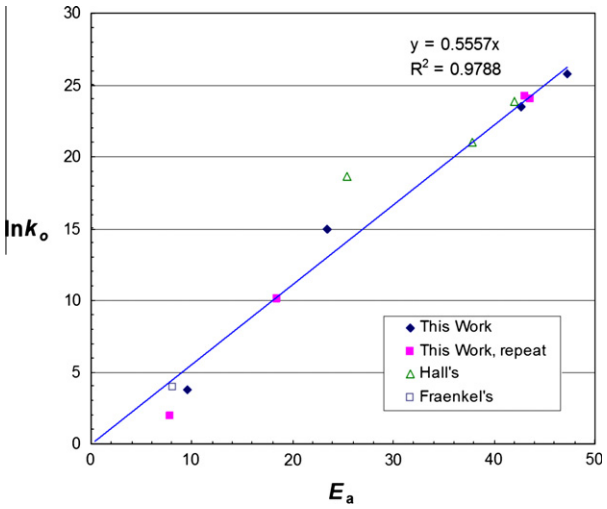

Fig. 13. Correlation between $\ln k_o$ and E_a (kcal/mol) values for the solid acids in Table 1 and for Fraenkel's SZ (Ref. [14]).

Next, we derive the correlation between H_0 and $\Delta S^{\ddagger}$. This is implicit from Eqs. (16), (17), and (22), through equating k of Eq. (22) with k_{efx}. For a constant k_{efx} (for a set of acids of various strengths, as in HAT),

$$\frac{\Delta S^{\ddagger}}{R} - \varepsilon_{ox} - 2.3H_0 \approx Const.', \tag{25}$$

and therefore, $H_0 = 0.219\Delta S^{\ddagger} - Const.''$. This equation is verified by plotting H_0 against $\Delta S^{\ddagger}$, as shown in Fig. 14 ($Const.'' = 7.2$). At the suggestion of an anonymous reviewer, we wish to make it clear that the correlation between H_0 and $\Delta S^{\ddagger}$ is not a novel kinetic finding of the current study, and it is to be expected in view of the fact that a compensation effect between $\Delta S^{\ddagger}$ and $\Delta H^{\ddagger}$ is known to occur in many reactions.

4.5. How HAT compares with kinetics of reactions catalyzed by liquid superacids

In the current work, we advocate that ε_x ($x \ll 1$) of an acid-catalyzed reaction of a very weak base can be correlated with H_0 through Eq. (18) (or (1)). Thus, under the kinetic requirements of the proposed correlation, H_0 is expected to be a linear function of $E_a/2.3RT_x$ with slope 1. For isobutane conversion, arbitrarily setting

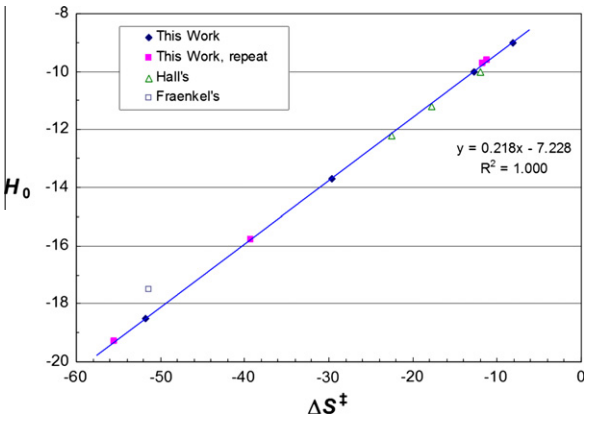

Fig. 14. Plot of H_0 vs. $\Delta S^{\ddagger}$ for the solid acids in Table 1 and for Fraenkel's SZ (Ref. [14]).

$x = 0.005$ defines the HAT for the (arbitrarily) chosen reactant flow (as F/W, see above), and we have calibrated our isobutane conversion test against H_0 values obtained by Hall's group. The controversy on the adequateness of the measurement of H_0 in solids and even the legitimacy of the H_0 concept in the case of solid acids nevertheless remains unresolved. In Section 4.3, we showed that 1 g catalyst (the basic measure unit of the catalytic function in HAT) can be reasonably correlated with the amount of the actual acid sites of interest ("the strongest") for zeolites and SZ, hence the conversion results can be roughly translated to TOF values. In Section 4.4, we have further suggested that this can allow interpretation of the kinetic data in terms of activation parameters of the transition state. The extent of the shift of $\Delta S^{\ddagger}$ to more negative values is interpreted as reflecting an increase in order in the protonated isobutane, as transition state, compared to the ground state, and, as expected, HAT-derived $\Delta S^{\ddagger}$ directly correlates with HAT-derived H_0. One may argue, of course, that the correlation is inherently deficient in being based on H_0 values derived by experimental means considered by many as unacceptable.

If HAT could be performed for liquid superacids, the above difficulty would have been removed; unfortunately, this is unfeasible. However, the internal *logic* of the HAT, with the kinetic development of the current study, can be examined with another, suitable test reaction that can be performed in the liquid state, with liquid superacids. Then, ε_x values for $x \ll 1$ (e.g., $\varepsilon_{1/2\%}$) could be correlated with H_0 values that are undisputed as being true representatives of acid strength. Here, we ask two questions: 1. Is ε_x correlating with H_0 of liquid acids in the expected fashion? 2. Can Eq. (18) (or (1)) be verified for liquid superacids? The effort taken for answering these questions seems very justified. We have chosen, as acidity test, the old work of Brouwer and van Doorn [44] who studied, by ^{1}H NMR spectroscopy, the cleavage of protonated methyl neopentyl ketone (MNK, 4,4-dimethyl-2-pentanone) as obtained by dissolving MNK in various strong acids and superacids. They measured the reaction rate as a function of temperature and found the rate at constant temperature to increase with the strength of the acid (but without correlating the results with H_0!). Each starting reactant solution contained 1.4 mol/l of $MNKH^+$, and the conversion to product was small enough to assume about constant reactant concentration throughout the measurement of the reaction rate. Brouwer and van Doorn presented their results as k (s^{-1}) vs. temperature and provided the calculated activated parameters based on the transition state theory. We have repeated their analysis in order to check the reported data and for obtaining higher accuracy. (This was done, using an Excel® spreadsheet, through

Table 6
Data of Brouwer and van Doorn on protonated-MNK cleavage, re-analyzed.[a]

No.	"Solvent"	T (K)	$-\ln k$[b]	$\ln k_o$[b]	E_a[c]	$T_{1/2\%}$ (K)	$\varepsilon_{1/2\%}/\ln 10$	k[b,d] $\times 10^5$	$\Delta G^{\ddagger}$[c,d]	$\Delta S^{\ddagger}$[e]	H_0[f]	H_0[g]
1	H_2SO_4, 98.1%	372.2	10.38	38.45	36.0	415.8	19.0	0.0476	30.2	16.9		−10.5
		377.4	9.85									
		388.7	8.33									
2	HSO_3F	357.1	11.79	43.18	38.8	404.5	21.1	0.0859	29.8	26.2	−15.8	−15.07
		377.8	8.65									
		387.3	7.54									
3	HSO_3F–SbF_5, 5:1	359.6	9.74	31.67	29.5	402.5	16.1	0.835	28.3	3.4	−20.8	−20.7
		367.1	8.86									
		377.5	7.73									
		388.8	6.63									
4	HSO_3F–SbF_5, 1:1	347.0	10.09	30.49	27.9	393.7	15.5	2.57	27.5	1.1	−21.3	−22
		357.3	9.03									
		367.5	7.86									
		377.4	6.84									
5	HF–SbF_5, 8.9:1	331.2	8.81	27.06	23.5	367.1	14.1	52.1[h]	25.5	−5.7	−22.8	−23
		344.6	7.44									
		357.5	6.17[h]									
		371.1	4.96[h]									
6	HF–SbF_5, 1:1	287.4	8.70	20.24	16.5	326.6	11.1	1718	23.1	−19.2	−25.8	−26
		298.1	7.84									
		307.2	6.97									
		312.2	6.45									
		317.2	5.99									

[a] Ref. [44]. Ratios in the acids are molar.
[b] k in s^{-1}.
[c] kcal/mol.
[d] At 70 °C.
[e] cal/(mol K).
[f] Predicted, or "smoothed".
[g] Literature values based on Refs. [1,2]; value for HF–SbF_5, 1:1 estimated as average between values proposed by Olah et al. (Ref. [2], Fig. 1.3 therein), and by Jost and Sommer (Ref. [45]).
[h] Values corrected; original k's obviously in error, being an order of magnitude smaller.

mathematical calculation and graphical analysis based on a least-square regression; such an analysis obviously could have not been performed by the above authors). The results, presented in Table 6, are similar to those reported but not identical, and Fig. 15 demonstrates the extent of agreement between the original kinetic data and the parallel recalculated data. As in the case of HAT (Fig. 13), a compensation effect is observed between ln k_o and E_a, with intercept zero; T_{iso} is 459 K. We have also extracted $T_{1/2\%}$ and $\varepsilon_{1/2\%}$ data (here, for 1/2% conversion per s) by interpolation or extrapolation of the corresponding Arrhenius plots, as presented in Fig. 16. (This Figure is comparable to Fig. 4.)

It should be noted that MNK is a strong base and thus, is completely protonated in strong acids having H_0 values of −10 or lower. The rate-determining step in the cleavage reaction can be assumed to be the *pseudo* first-order protonation of protonated-MNK. Indeed, Brouwer and van Doorn postulated that a $(MNKH^+)H^+$ dication may act as transition state in the acid-catalyzed cleavage of $MNKH^+$. Thus, the reaction is not represented by Eq. (2), but rather by the parallel equation

$$BH^+ + H^+ \Longleftrightarrow (BH^+)H^+. \quad (26)$$

As known, BH^+ carbocations are very weak bases and some are used as Hammett indicators for measuring H_0 below −17 [1,2]. We thus can safely assume that only a small portion of BH^+ is protonated and, of course, the acid is in large excess. Therefore, the kinetic analysis as developed for HAT can be applied here as well. Fig. 17 demonstrates that Eq. (18) (Eq. (1)) is adequately followed over a range of acidities, from H_0 of −15 to −26. Here, $Int_{1/2\%}$ is −36.85, meaning that $MNKH^+$ is a much weaker base than isobutane and can, theoretically, probe acid strength down to about $H_0 = -37$. The fit with the straight line (Fig. 17) is less satisfactory for H_2SO_4(98.1%) (Table 6), perhaps due to inaccuracies in the kinetic measurements [44], and, therefore, this case was omitted. It is thus indicated, through the analogy with the liquid-phase $MNKH^+$ acidity test, that the theoretical basis of HAT is sound. However, the analysis of the MNK work cannot provide support to the assumption that the particular H_0 values assigned to the solid acids are valid; it only confirms that the relative *span* of the H_0 values in the solid acids is as could be expected.

Fig. 18 presents plots of H_0 vs. $\Delta S^{\ddagger}$ for literature H_0 values and for "smoothed" H_0 values (Table 6) according to the kinetic prediction based on the activation parameters. Smoothed H_0 values are within the experimental error of the measured (or estimated) H_0 values. The smoothed H_0 vs. $\Delta S^{\ddagger}$ straight line follows the expression as derived above (Section 4.4) based on Eq. (25).

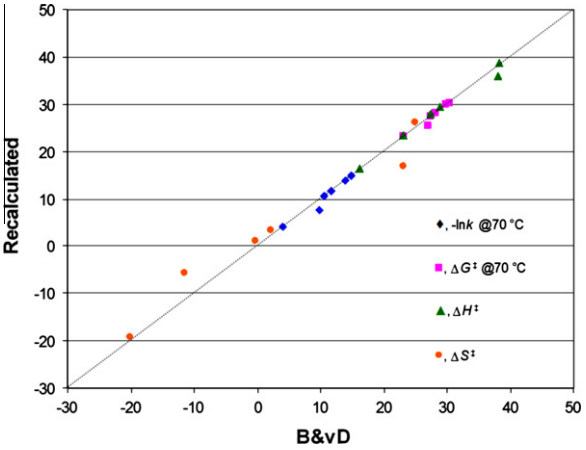

Fig. 15. Comparison between recalculated and original kinetic parameters of the cleavage of MNK (B&vD – Ref. [44]).

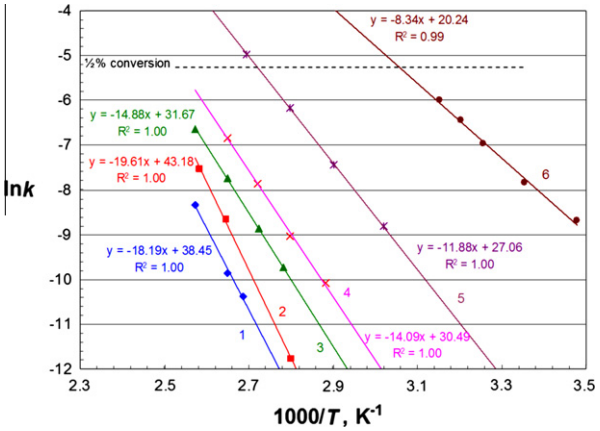

Fig. 16. Arrhenius plots for $MNKH^+$ cleavage (Brouwer and van Doorn, Ref. [44]). The kinetic data are those listed in Table 6 for the respective liquid acids.

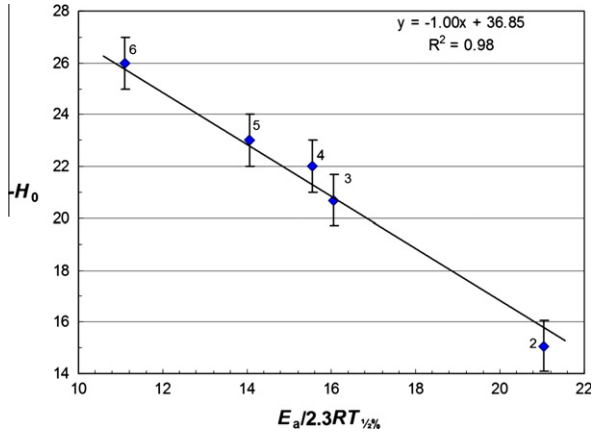

Fig. 17. A plot of $-H_0$ vs. $E_a/2.3T_{1/2\%}$ ($=\varepsilon_{1/2\%}/\ln 10$) for the liquid superacids in the catalytic cleavage of $MNKH^+$ (Table 6). Note the comparability of the straight line obtained with that of Fig. 5.

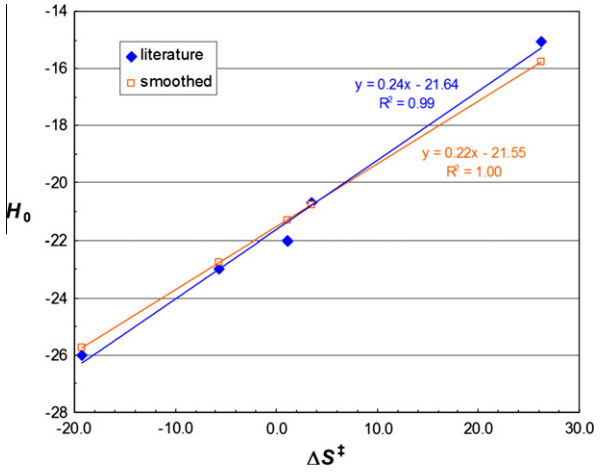

Fig. 18. Plots of H_0 vs. $\Delta S^{\ddagger}$ for literature (full diamond) and smoothed (empty square) H_0 values (Table 6).

5. Discussion

5.1. Superacidity and alkane conversion

Hammett's H_0 is related to protonation, hence to the strength of the Brønsted acid function (or the proton). H_0 therefore corre-

lates with the activity of the proton (always in its solvated form), and, specifically, with the activity coefficient, f_{H^+} that varies much more strongly than concentration (C_{H+}, or [H^+]) at high proton activity (a_{H^+}). H_0 thus is not affected by the *kind* of anion compensating the positive charge of the proton. Olah has frequently emphasized [2,46,47], following Gillespie and Peel [1], that the definition of superacids as acids with H_0 lower than −12, although very useful, is rather arbitrary. Thus, the change of acid strength is always continuous and therefore, the borderline between "just strong acids" and superacids does not bear any theoretical meaning. It appears that a single function is responsible for acid strength and it most plausibly relates to the anion *size*. In discussing fluorosulfonic acids, Olah [31] pointed out that the dramatic increase in acidity is due to the formation of "*large complex fluoroanions facilitating dispersal of the negative charge.*" Likewise, Umansky and Hall stated [10] that "*acidity is enhanced as the size of the anion (the conjugate base in which the electron is delocalized) is increased.*" It can thus be also said that acid strength is intimately related to the anion size *in all acids*, weak and strong, and anion size hierarchy should be parallel to acidity scales. In the weaker acids, such as the simple mineral acids HCl and HBr, in aqueous solution, anions are relatively small but the acid strength ranking still follows the anion size (so, for instance, at the same concentration, HBr is a stronger acid than HCl) [2,23,48]. HSO_3F is a much stronger acid ($H_0 = -15.07$ [1]) by virtue of the SO_3F^- anion being considerably larger than a monatomic halide; acids even stronger than simple Brønsted acids are obtained by combining Brønsted with Lewis acids [1,2] thereby creating bigger anionic entities through the attachment of the Brønsted acid conjugate base (with a negative unit charge) to the Lewis acid (neutral); this happens, for example, in the HCl-$AlCl_3$ adduct ($H_0 \sim -16$ [31]) and in Magic Acid®, HSO_3F-SbF_5 ($H_0 \sim -18.6$ for the system with 14–20%mol SbF_5 [1]). In typical solid acids, such as H-zeolites, the locus of electron dispersion around an anionic center [e.g., $(-O)_4Al^-$ center] defines an "effective anionic size"; as this effective size increases, e.g., by increasing the silica-to-alumina ratio, the intrinsic acidity (that is, acid strength per site) is enhanced.

To further advance the above ideas, one may argue that as the anionic size of Brønsted acids increases, so does the chemical potential of the proton, relating to the logarithm of f_{H^+}. This may be attributed to the lack of electrostatic compatibility between the cation and anion as their size difference grows, creating ionic repulsion effect [49] that, in the superacidity region, causes f_{H^+} values to skyrocket. As a result, H^+ can then attack any charge density, even the very weak one of C–C and C–H σ-bonds that are stabilized by very strong bonding due to a particular effective overlapping of atomic orbitals. By doing so, in spite of the chemical difficulty, the proton becomes "solvated" by a large molecular species thereby reducing the size difference between its own size (now considerably larger) and that of the big anion; this relieves interionic electrostatic repulsions [49] and decreases the chemical potential of the proton (or its Gibbs free energy). In terms of the activated complex of the transition state, a stronger acid, with larger anionic size, would cause $\Delta S^{\ddagger}$ to decrease, and for the strongest acids, become negative, as a result of more order in the transition state of a "solvated" proton (or a protonated base) compared to an "unsolvated" proton and a free base. In contrast, simple mineral acids (e.g., dilute sulfuric acid), under mild conditions, can only protonate C=C π-bonds in hydrocarbons, thereby yielding stable carbenium ions. In other words, there is not enough thermodynamic driving force, and need, for the proton to attack σ-bonds. The correlation between f_{H^+} and H_0 is straightforwardly derived from the H_0 definition (see above). For a constant proton concentration, C_{H^+}, or [H^+], and assuming about constant f_{BH^+}/f_B ratio, we have Eq. (11), and it is thus clear (and well known) that, with such an assumption, an increase in f_{H^+} causes a decrease in H_0, which translates to stronger acidity.

We have established the effectiveness of HAT as a consistent, reliable probe of strong acidity in solid acids, subject to the validity of the assumptions and approximations on which this test method is based. The method was introduced by Hall's group [11] in 1991; Fraenkel [14] extended it to SZ, and by employing a kinetically derived expression relating H_0 to $E_a/T_{1/2\%}$, inferred that SZ can possess H_0 of *ca.* −17.5. In the present work, HAT was used systematically for different strong solid acids varying considerably in their acid strength. We have repeated our work a year later with very good reproducibility ("repeat", Table 1); our results are also consistent with those of the older studies. Furthermore, LZ-Y82 (a high-silica HY) gave about constant H_0 values whether obtained by HAT or by a "simulated HAT" based on extrapolation of high conversion data of older literature from the 1980s. The robustness of the test emphasizes its usefulness in ranking solid acids by their acid strength. In the current work, for the first time, SZ was subjected to HAT alongside H-zeolites under the exact same strict set of reaction conditions of isobutane conversion, which defines this acidity test; the acid strength hierarchy ($-H_0$) was found to be: SZ(18) ≫ HM(14) > HZSM-5(10) ≈ HY(9). This hierarchy is supported by spectrophotometric measurements [11] (of HM and HY) and by Hammett indicator measurements based on color change (for SZ and HM). Moreover, in measuring the acid strength of a HY sample similar to ours (SiO_2/Al_2O_3 = 4.73, 87.5% H-form), Otouma et al. [50] demonstrated that about 15% of the acid sites have $H_0 < -8.2$. Our results are in agreement with this finding. For HY samples of similar characteristics and a HM sample with 92%mol H^+, Ikemoto et al. [51] claimed that the acid strength is distributed in the $-H_0$ range of 8.2–10.8. As suggested in the present work, H_0 of about −10 may involve 2–3% of the H^+ sites, as the strongest. However, 20% or more sites may protonate anthraquinone. According to our study, HY is not significantly different from HZSM-5 in acid strength, but has considerably higher H_0 than HM. HM thus should be a much more active catalyst than HY in Brønsted acid-catalyzed hydrocarbon conversions. Indeed, Benesi found [52] this to be the case in *n*-alkane cracking and in toluene disproportionation, both reactions known as typical Brønsted acid catalytic reactions; Pd or Pt versions of the above zeolites preserved the same activity order in alkane isomerization and hydrocracking, as found by Burbridge et al. [53].

5.2. Acidity measurements of solids by MAS NMR

The acid strength of zeolites and sulfated zirconia has been studied by MAS NMR spectroscopy. Basically, two approaches have been followed. In one, the solid acids are measured directly using ^{1}H NMR, as done by Pfeifer et al. [54], Armendariz et al. [55] and Reimer et al. [5]; in the other, an indirect measurement, using ^{13}C, ^{15}N, ^{31}P and ^{19}F NMR, is conducted employing probe molecules and examining their ability to become protonated in the presence of the acid. We shall come back to the direct measurement in a while, but first deal with the indirect NMR study as was especially developed and advanced by Haw and coworkers. As in the case of the work of others, such as Adeeve et al. [7], mentioned in the Introduction section, the use of probe molecules for spectroscopic studies should be treated with caution especially when trying to provide evidence on acid strength. Two problems are in particular interfering with the acid strength measurement – the base strength and the amount adsorbed. In some cases [7,56], the probe molecule was a too strong base and was used in excess amount, compared to the Hammett indicator method. We have mentioned above that under such conditions, the base may not equilibrate with the acid sites, and adsorption may adversely affect the acid strength of the remaining sites. Another potential problem is

adsorption itself, especially with aromatic bases, which may obscure or block acidic sites. With all the above reservations, we shall still examine Haw's results.

Haw's group arrived at the sweeping conclusion that "*zeolites are not superacids*" [57] thus reversing earlier literature in which "*zeolites were most often classified as superacids, the solid equivalent of magic acid*." A correction is immediately in order: Even if zeolites are superacids, they are definitely not "*the solid equivalent of magic acid*" and claiming it does not reveal much understanding of solid acids and of acidity strength; Magic Acid® may be a million times (or more) stronger acid than a zeolite while the latter solid may still be a superacid! However, a major difficulty with Haw's work is that he used mediocre solid acid zeolites to prove his point: HY with SAR = 2.5 (a calcined NH_4Y, as in the present work) and HZSM-5 with SAR = 19–21 [58]. It is very well known and found in full agreement with the current work and with the relevant cited literature [10–12], that zeolite acidities are strongly influenced by the silica-to-alumina ratio, with the higher ratios giving stronger acidity. It is not clear why Haw chose HY with the lowest SAR to draw conclusion on zeolite acidity *in general* (whether in the superacid region or not). However, our results are in full agreement with his NMR evidence. Haw showed, in an otherwise beautiful piece of study, that his NMR system is capable of tracking base protonation on HY and HZSM-5 when the base is very strong (such as *para*-fluoroaniline, pK_a = +2.4, and *para*-nitro(^{15}N)aniline, pK_a = +0.99), but no protonation is detected with bases of similar structures, which are Hammett indicators (i.e., extremely weak bases) with pK_a of −12.4 and −11.4, respectively (see Table 4). We are pleased with this indirect confirmation that our similar HY sample has $H_0 > -11$ and we found this value to be −9 or −10. We are likewise pleased with Haw's HZSM-5(SAR = 19) with $H_0 > -11$ even though our own HZSM-5 sample, that still exhibited higher H_0, had SAR = 36. Unfortunately, Haw did not extend his NMR work to dealuminated HM (MOR) and to SZ. We thus conclude here that the NMR study of Haw et al. and the HAT work reported here are in full accord with each other; but this does not mean that zeolites are never superacids. In fact, our analysis of the catalytic work of McVicker et al. [12] in isobutane conversion (see above) indicates that the LZ-Y82 sample (HY; SAR = 2.7) they used may be marginally superacidic (Table 3). Similar high-silica HY samples of Hall's group [10,11] could have been approximately as strong as 100% sulfuric acid. Some dealuminated HM samples appear to be true solid superacids (see above).

Pfeifer et al. [54] were the first to detect the acidity of zeolites by ^{1}H NMR, and for a series of acid zeolites including HY, HZSM-5 and HM, they found a characteristic resonance peak at δ 4.1–4.4 ppm (TMS, δ = 0). No details were provided on the specific samples used (such as SAR). Riemer et al., in a similar study but involving SZ, found the acidic H^+ resonance at 5.85, 1.5 ppm downfield from the H^+ of ZSM-5, and concluded, therefore, that SZ is a superacid [5]. Armendaris et al. [55] and Mastikhin et al. [40] reported the same results, but the former group, in addition, correlated the 5.8 ppm peak with an infrared absorption band (of DRIFT) at 3300 cm^{-1}, believed to reflect strong Brønsted acidity. In accord with this conclusion, these authors reported the activity of SZ in deuterium exchange with benzene-d_6, implying benzene protonation, at room temperature. Haw, using ^{13}C MAS NMR [59], detected $C_6H_7^+$ related to benzene–$^{13}C_6$ in frozen Magic Acid® at 83 K, and in $HBr/AlBr_3$ at 77 K and higher, but no such protonation was observed with HY at any temperature above 100 K. Even though Haw's work cannot be directly correlated with the work of Armendariz et al., one may claim, based on the evidence provided, that SZ is a stronger acid than HY.

While not comparing NMR spectra of zeolites with those of SZ under similar measurement conditions, to gain evidence on their relative acidities, Haw did perform a limited NMR work on the protonation of trimethylphosphine and of pyridine–^{15}N in the presence of SZ, using ^{31}P NMR and ^{15}N NMR, respectively [56]. The results were not interpreted as providing direct evidence on the acid strength of SZ. But we also have to caution, as before, that the meaning of adsorbed strong bases ($P(CH_3)_3$, pK_a = +8.65; Pyridine, pK_a = +5.23) over a superacid solid, as acidity probe, is, at best, compromised. In the standard Hammett indicator tests, as used by us (see above), a base over 10^{13} times weaker than the above bases was protonated by about 5% of the available acid sites (estimated, see above); in contrast, in Haw's work, the lowest base loading applied corresponded to ~100% of the available acid sites.

5.3. Acidity and alkane conversion mechanisms

5.3.1. General considerations

The finding of the current study that SZ is a strong superacid parallel, in H_0 terms, to Magic Acid® and to HCl–$AlCl_3$, is supported by *n*-pentane conversion studies at ambient conditions in the liquid phase. It also reconfirms the work and claims of Hino and Arata [3,15]. However, this finding sharply contrasts with literature's conclusions – based on spectroscopic and calorimetric analysis of strongly adsorbed probe molecules – as mentioned above, according to which SZ is interpreted as being a strong acid, with a strength that parallels that of common H-zeolites, but *not* a superacid. It is noteworthy that, unlike SZ, no zeolite has so far been found to exhibit room-temperature *n*-pentane conversion activity (except for HM as reported now, see above); moreover, the activity and selectivity of SZ in this reaction is similar to those of known superacids. There is overwhelming evidence in the literature, supporting a Brønsted acid-catalyzed carbocation mechanism in the low-temperature conversion of alkanes, such as butane and pentane, over strong superacids. It thus seems implausible to invoke [7,13] a different mechanism for SZ, in spite of the fact that SZ behaves very similarly to known superacids; moreover, invoking this just because some spectroscopic/calorimetric studies, possibly due to their own inherent deficiencies and limitations (see above), failed to depict the strength of this acid, is farfetched. Furthermore, a redox mechanism based on the oxidizing power of the sulfate group, or sulfuric acid, as proposed [13] does not appear to be supported by our study. Evolution of SO_2, indicative of oxidation, was indeed encountered after many hours at room temperature in the conversion of *n*-pentane by concentrated sulfuric acid, but not in the presence of SZ, alone or with added H_2SO_4. GC and GCMS analysis only revealed skeletal transformation products with unchanged carbon oxidation state.

As shown above – and at odds with interpretations of results of spectroscopic or calorimetric measurements as reported so far – SZ is a much stronger solid acid than any H-zeolites (that it may resemble in acid strength by some spectroscopic observations) both by the direct H_0 tests (using indicators) and based on activity/selectivity differences in hydrocarbon transformations. More specifically, in this work we have addressed the unjustified literature claim [32,37] that ammonia or amine adsorption and calorimetry may provide evidence on acid strength of solid acids; in particular disturbing is the attempt to "show" that gas-phase proton affinity of amines does not scale with solution-phase acidities, when the particular literature cited as source of the relevant data claims the exact opposite. The process of surface adsorption of a (relatively) strong base on a solid acid – and especially the heat evolved, comprising several steps, some being enthalpy-compensating – is a complex chemical change; in contrast, a simple, first-order reaction of a very weak base in contact with a solid acid, through protonation as a rate-determining step, is a straightforward manifestation of acid strength. We have tried to support this argument through an analogy with a liquid-phase reaction involving liquid superacids of known H_0, to demonstrate that the pro-

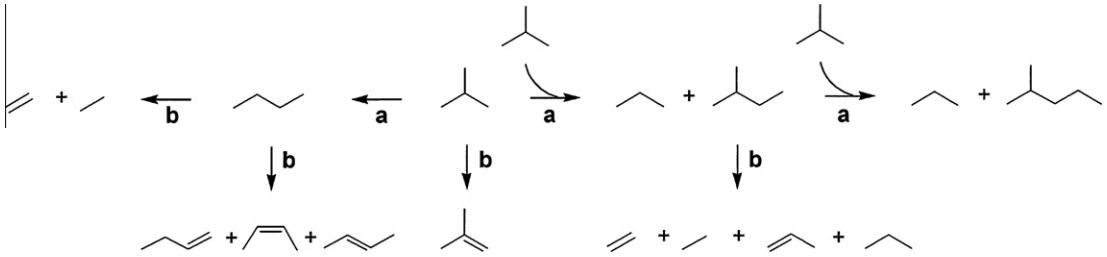

Scheme 2. Plausible reaction network in isobutane conversion over strong solid acids.

posed kinetics of the above process, as developed for HAT, is valid and sound. For this, we employed the old work of Brouwer and van Doorn [44] on the cleavage of protonated methyl neopentyl ketone (a very week base), and shown a nice compliance with Eq. (18) (or (1)) (Fig. 17). A similar scaling of acidity with the kinetics of weak base conversion is shown in HAT (Fig. 5).

The distinction of SZ from the zeolites is also apparent from the product distribution pattern in isobutane conversion, even though superacidic HM gives only slightly different pattern compared to SZ. The major change occurs between HM ($-H_0$, ~14) and HZSM-5 ($-H_0$, ~10). We, therefore, can attribute the product distribution change to a transition from "strong acid" (i.e., $-H_0 \leqslant 12$) to "superacid" ($-H_0 > 12$). The product distribution pattern agrees with a general isobutane conversion mechanism as proposed in Scheme 2. Here, "**a**" routes, corresponding to superacidic isomerization and disproportionation pathways, are distinguished from "**b**" routes due to weaker (albeit quite strong) acidity catalyzing dehydrogenation and cracking instead. For superacids, **a** ≫ **b** whereas for non-superacids, **b** ≫ **a**. This is further illustrated in Scheme 3 presenting the various single-step reactions of isobutane starting from a carbonium ion (superacid) and from a carbenium ion (non-superacid). The latter ion can be produced either by the collapse of a previously formed carbonium ion through isobutane protonation by Brønsted acid sites (e.g., *via* eliminating dihydrogen [2]), or by hydride abstraction occurring over Lewis acid sites (at elevated temperature). Methane is not expected as product of either mechanism; rather, it is most probably the product of a thermal, free-radical cracking mechanism [12] as presented in Table 7. In this Table, the first two reactions are the most effective at elevated temperatures; coupling reactions become important only with high radical concentration and at low temperature [12,25]. Since H_2 is obtained also by acidic dehydrogenation involving carbenium ions, and so are C_3 and C_4 olefins, CH_4 seems the only clear marker of the non-acid, thermal route. Indeed, increased methane concentration is always seen at elevated temperatures, especially above about 450 °C. However, as shown and pointed out by McVicker et al. [12], weak acids that operate only at very high reaction temperature, thereby being inside the free-radical thermal regime, may trigger radical formation and/or stabilize radicals; they thus may cause isobutane conversion to occur more readily even when not involving catalytic acid sites.

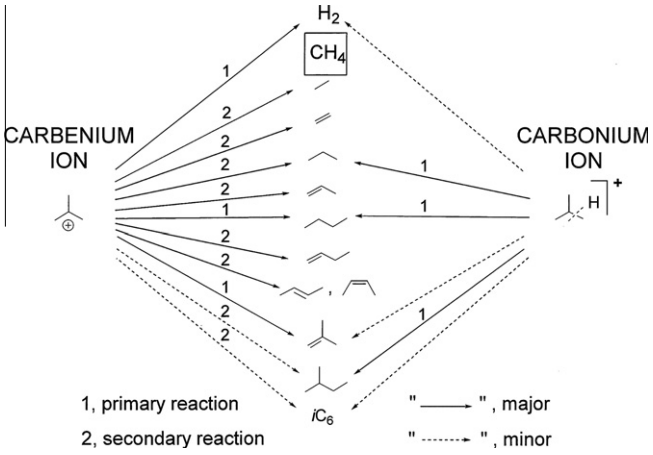

Scheme 3. Single-step reactions – primary and secondary – in acid-catalyzed isobutane conversion.

The extensive formation of methane, olefins and H_2 at elevated temperatures, with the molar concentrations being $[CH_4] \approx [C_3H_6]$ and $[H_2] \approx [C_4H_8]$, due to thermal cracking pathways, offers a facile alternate route to the Brønsted acid-catalyzed pathways. But Lewis acid sites, in addition to facilitating formation and perhaps stabilization of radicals, may form carbenium ions by (high-temperature) hydride abstraction. The outcome of diminishing the extent of Brønsted acidity-related reactions among all reactions involved in the isobutane conversion, is decreased values of $T_{1/2\%}$ and E_a; the relative effect on E_a is stronger and the consequently smaller $E_a/T_{1/2\%}$ values thus decrease calculated H_0 values, falsely reflecting stronger acidity than in reality. This is because in the kinetic development, the rate-determining step is assumed to be the isobutane protonation reaction (see above); the assumption is compromised when the reaction is not entirely Brønsted acid catalyzed. We therefore conclude, based on the experimental evidence of the present study, that HAT cannot be used reliably above about 450 °C, and in terms of H_0, this means that the weakest solid acids that can effectively be measured by HAT should have H_0 of −8 or less. On the other extreme, H_0 of about −20 is expected as the practical upper limit of this acid strength test.

5.3.2. Presence of olefins in the reactant feed

The role of olefins and olefin impurities in the mechanism of the catalytic skeletal transformation of saturated hydrocarbons in the

Table 7
Various radical reactions that may be involved in isobutane conversion.

1	Dealkylation (fragmentation)	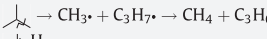
2	Dehydrogenation	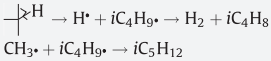
3	Alkylation	$CH_3\bullet + iC_4H_9\bullet \rightarrow iC_5H_{12}$
4	Hydrogenation	$H\bullet + C_3H_7\bullet \rightarrow C_3H_8$
5	Coupling	$CH_3\bullet + CH_3\bullet \rightarrow C_2H_6$ $C_3H_7\bullet + C_3H_7\bullet \rightarrow C_6H_{14}$

presence of strong acids is still controversial even though it has been first recognized many decades ago [29].

Our isobutane gas reactant (as 10%, at 99.9% purity, in 90% He, at 99.999% purity) as well as the He carrier gas (99.995% purity) had no GC-detectable olefins. Additionally, the gas feed was passed over a zeolite (HM) trap prior to being brought in contact with the catalyst. A similar purification method was reported by Dumesic's group [9] who stated that no olefin impurities were present in their feed. Xu and Sachtler applied a more rigorous purification procedure in the case of *n*-butane isomerization, and estimated that the olefin-to-paraffin ratio in their *n*-butane feed was as low as 10^{-15} [39]. In both literature cases, the starting reactant had 5- to 10-fold higher impurity level in the as-received reactant gas compared to our gas feed. Based on the similarity of the reaction network at ~150 °C between our work and the literature, coupled with the fact that our SZ sample was not more active than samples of similar chemical and structural characteristics as employed by the other researchers, we strongly believe that olefin impurities did not play role in our study. Xu and Sachtler [39], in an *n*-butane isomerization study with deuterated SZ, did not detect any molecules with more than one ^2H atom; they interpreted this finding as indicating that olefin molecules at the catalyst surface (assumed to be formed during the reaction) are "tied up" at the surface. The fact that SZ is active in butane isomerization at 150 °C without olefins present in the feed, led Dumesic's group [9] to propose that SZ is capable of generating olefins *in situ* to initiate a surface chain reaction. They gave an effective review of the literature relating to the initiation step, i.e., whether occurring through alkane protolysis (initially forming a carbonium ion), or proton addition to an olefin (yielding a carbenium ion), or otherwise. Carbonium ions are generally believed to only be more facile precursors of carbenium ions in catalytic hydrocarbon conversions; the latter ions are considered as the actual reactive intermediates causing the reaction, i.e., alkane skeletal transformation. The carbonium-to-carbenium ion conversion, in its simplest mode, happens through either H_2 or CH_4 elimination [2]. Methane has not been reported in low-temperature alkane isomerization over SZ, but Dumesic's group claimed that H_2 was produced along with isomerization products in both *n*-butane and isobutane reactions over SZ [9]. They measured a H_2/nC_4 molar ratio of 0.002 in the isomerization of isobutane (100% in feed, 150 °C, 6.2% conversion). While this could be an indication of protolysis of isobutane, it, perhaps, could also be the result of some minor dehydrogenation activity generating coke precursors, as mentioned by the authors.

It is plausible that if SZ is a very strong acid and if olefin impurities are absent, then at low temperatures, the alkane reactions may proceed through initial H^+ attack on a C–H or C–C σ-bond of the alkane to yield a carbonium ion. It is not apparent, though, that this necessarily should lead to protolysis through H_2 or CH_4 elimination and the concomitant generation of carbenium ions as the actual reactive intermediates. In other words, the necessity of carbenium ions in the alkane conversion mechanism under extreme acid strength may be put in question.

5.3.3. Postulated detailed mechanism of the isobutane conversion by strong acid catalysis

The conversion of isobutane by the strongest acids under the HAT conditions clearly indicates two different primary reaction courses – isomerization and disproportionation [29]. In the first, a methyl shift apparently occurs intramolecularly, and it may involve a monomolecular mechanism. The second course is that of intermolecular methyl shift, involving two isobutane molecules. Kinetically, such

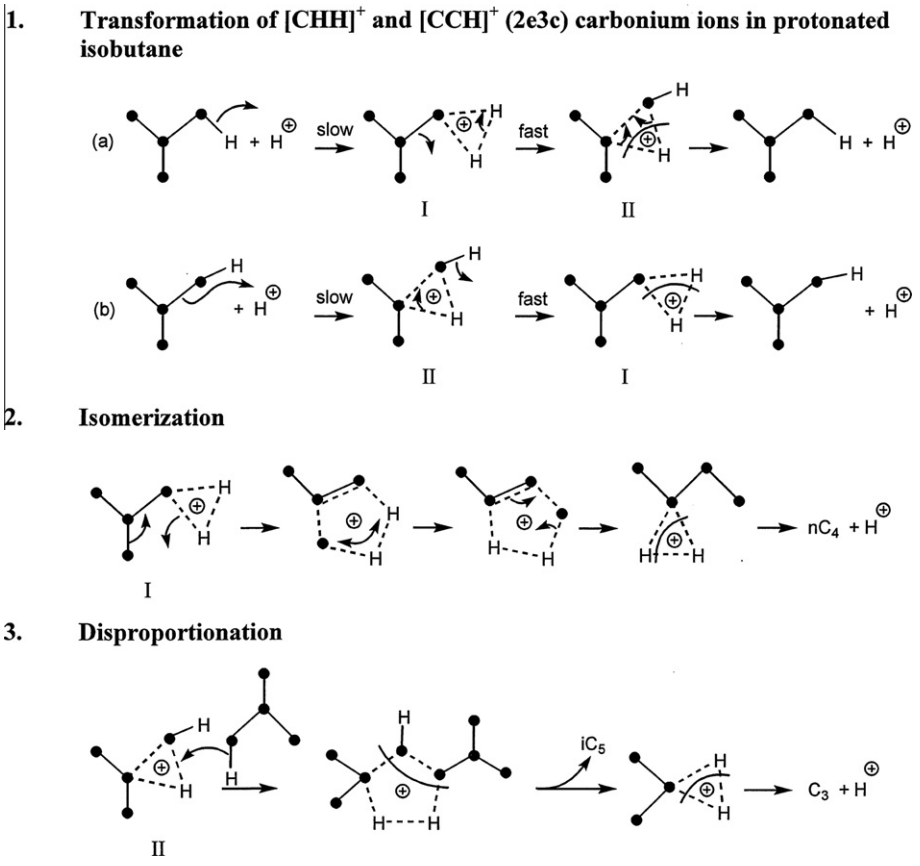

Scheme 4. Superacid-catalyzed isobutane conversion: A postulated mechanism. (Dots represent carbon (CH_x) groups; bent lines pass through bonds to be ruptured during the splitting of molecular/ionic fragments; bent arrows show electron shifts; bent double arrow symbolizes the equivalency of the two positions pointed at in the three-dimensional, 6e5c$^+$ "pentonium" ion.)

a bimolecular reaction may or may not be first-order, but we assume that it is. An anonymous reviewer has raised a legitimate concern on the possibility that isomerization and disproportionation may follow two different reaction mechanisms, in regard to protonation, which may render HAT meaningless since the two reaction courses cannot be separated from each other. The reviewer claimed that, unlike in the monomolecular mechanism, in the bimolecular one the surface proton is not directly involved because it was transferred to a surface hydrocarbon species *prior* to the bimolecular step. We believe, however, that the bimolecular step may not be rate-limiting in the overall reaction. Thus, in the current analysis, a further assumption is made that in both isomerization and disproportionation, the initial protonation of isobutane is the rate-limiting step. A plausible mechanism for the overall isobutane conversion is delineated in Scheme 4. Protonation may occur, as the slow step, on either a C–H or C–C bond (or both), creating the initial carbonium ion, either I or II. These $C_4H_{11}^+$ cations may equilibrate fast by an electron (bond) shift, as described. Both carbocations may fall back to isobutane and H^+ if not transformed or reacted otherwise. In isomerization, carbonium ion I (a $2e3c^+$ ion) is proposed to transform, through an addition of a β C–C bond, to a $[CCCHH]^+$ ($6e5c^+$) intermediate, or transition state, that undergoes skeletal rearrangement followed by collapsing to a new C–C bond and a carbonium ($2e3c^+$) ion that finally dissociates to *n*-butane and H^+.[2]

Disproportionation may occur through an attack of carbonium ion II on a C–H bond of a second isobutane molecule to form a $[CCCHH]^+$, $4e5c^+$ intermediate (or T.S.) that, in one possible scenario, can eliminate isopentane, thereby collapsing to a $C_3H_9^+$ carbonium ion; the latter ion subsequently deprotonates to release propane. Thus, it is plausible that both isomerization and disproportionation would have the same initial isobutane protonation as the rate-controlling step, even though the first reaction may be monomolecular whereas the second is necessarily bimolecular. It is, of course, possible that both reactions are bimolecular as has been suggested [60,61]; but Garin et al. [62], based on ^{13}C labeling studies, concluded that butane isomerization at low conversion (<30%) is monomolecular "*in accord with the superacidic properties of the catalyst* [SZ]". It is important to note that in the literature's mechanism for the bimolecular reaction of C_n alkanes ($n = 4, 5, 6\ldots$) [29,61,63,64], coupling of two C_n molecules to give "C_{2n}" is believed to form a $C_{2n}H_{2n+1}^+$ carbenium ion, e.g., $C_8H_{17}^+$ in the case of butane. In contrast, the C_8^+ carbocationic species proposed by us is a $C_8H_{19}^+$ "supercarbonium" ion (stage 3 in Scheme 4). Such a hyper-ionic structure is believed to uniquely represent an alkane disproportionation mechanism promoted by superacids since it avoids involving carbocations that can be created from or transformed to unsaturated hydrocarbons.

6. Conclusions

The acidity test based on 1/2% isobutane conversion devised by Hall's group [11] (hence "Hall Acidity Test") has been found to be a simple, reliable and powerful method for estimating the Hammett-acidity function of strong solid acids in the approximate H_0 range of −8 to −20, using the kinetic equation derived by Fraenkel [14]. Measuring sulfated zirconia (SZ) vs. common H-zeolites by this method, leads to the inevitable conclusion that SZ, when at its appropriate activated state, is at least three H_0 units below the strongest H-zeolite, HM, on the Hammett acidity scale, and is as strong as known strong liquid superacids, such as Magic Acid®. This conclusion is corroborated by other evidence: NMR [5], Ar-TPD [15], comparative product distribution of isobutane conversion, comparative liquid-phase *n*-pentane conversion, and Hammett indicator color change. SZ thus appears currently as the strongest unpromoted oxide solid superacid ever prepared. We speculate that what may make SZ so strongly acidic is a special sulfate-zirconia bonding that causes the locus of electron delocalization on the surface – or the effective surface "anion" size – to be as large as the effective size of the anion in strong molecular superacids, e.g., Magic Acid®. This effect may be influenced, if not created, by the single-digit nanocrystallinity of SZ (Fig. 2). We further speculate that the failure so far to recognize the strong superacidity of SZ in adsorption/calorimetry/spectroscopy studies, as mentioned above, may have been the result of one or more of the following: inferior SZ preparation, inadequate activation or handling (e.g., moisture control), poisoning effect of adsorbed probe molecules (too strong bases) on the strongest acid sites, or inherent limitations of the spectroscopic techniques used. Despite all the above, caution in interpreting the results of the present study is in order because of the legitimate doubts shed on the applicability of the Hammett-acidity function to solid surfaces, as well as the dependence of HAT on H_0 values measured by other methods. We nonetheless estimate that the H_0 values we derived in this work for the various solid acids studies are reliable within 1-to-2 H_0 units. Future efforts should focus on devising an acidity test, based on the reactivity of a very weak base, which can be convincingly applied to both liquid and solid acids. Such a test should not be based on bulk Brønsted acid neutralization as is often involved in spectroscopic and calorimetric measurements.

Acknowledgments

The study presented in this paper is based upon work supported by the U.S. Department of Energy under award Number DE-PS02-08ER08-17. Dr. Christopher L. Marotta skillfully conducted the TEM work. Dr. Richard Mackay offered valuable help in the XRD line-broadening Scherrer analysis.

Appendix A

A.1. Temperature effect on H_0

The acidity function represents the tendency of a Brønsted acid to donate a proton to a base, thus directly relating to f_{H^+}. Yet this very acidity function also represents the tendency of a base to *accept* a proton from an acid, which relates to pK_{BH^+} that is measured by experiment, and the concentration ratio $[BH^+]/[B]$ that is determined experimentally by measuring the spectrophotometric log *I* (of Lambert–Beer Law). f_{H^+} (the "ease of protonating") cannot be measured directly at high acidity, outside the pH scale, but according to a simplified electrostatic model, such as that of the Debye–Hückel theory [48], the left-hand side term in Eq. (11) – and therefore H_0, if *Const* is not a function of *T* – should depend not on $1/T$ (the Arrhenius effect), as does a kinetic constant *k*, but rather on $1/D_eT$, D_e being the dielectric constant of the solvent. We can learn on this effect by examining aqueous acid solutions: Since D_e decreases with increasing temperature, log f_{H^+} is responding only slightly to *T* (as can be seen for many acid solutions [48]) because

[2] This is a novel mechanistic concept, generally applicable to very strong acids, to be followed and developed further in subsequent publications. According to this concept, a carbonium ion, rater than collapsing to carbenium ion by eliminating a σ-bond (say, creating H_2) may instead attack a σ-bond (here, a C–C bond), thereby forming a highly reactive supercarbonium (penta-onium, or "pentonium") species, as intermediate or transition state. This electron-deficient $5c^+$ ion transforms internally, through pseudorotation (between square pyramid and trigonal bipyramid geometric conformations), thus providing a very feasible route to products. Such a mechanism avoids the energetically inconvenient "protonated-cyclopropane intermediate" as proposed by Brouwer (see Gates, Katzer and Schuit, Chemistry of Catalytic Processes, McGraw-Hill, New York, 1979, pp. 24–27, providing a very clear description of this concept). In the latter intermediate, assumed to facilitate *carbenium* ion transformation, bond angles are very small, creating considerable bonding strain, and the proton location is fuzzy as it does not follow conventional bonding concepts, such as in $2e3c^+$ and related structures.

D_eT is a weak function of T. The same is expected with lower-D_e, non-aqueous solvents.

In the literature, there have been attempts to estimate the temperature dependency of H_0 in terms of the indicator's "ease of becoming protonated", i.e., by measuring the effect of temperature on the indicator's measurable quantities I and pK_{BH^+}. The work covered aqueous sulfuric acid in the range 2–99%wt and was performed between 15 and 90 °C [65,66]. The effect was a function of the H_0 level. At high values, >−1.5, there was no T effect; but below −1.5, H_0 slightly increased with temperature; for example, with 98% H_2SO_4, H_0 changed from −10.38 at 15 °C to −9.74 at 55 °C [66]. Such a change ($dH_0/dT = 0.016$, assuming linearity) is smaller than that expected from the Arrhenius dependence at a parallel temperature, say 35 °C [$d(\log k)/dT = E_a/2.3RT^2$, e.g., 0.092 for E_a = 40 kcal/mol, roughly corresponding to $H_0 = -10$; see above]; it therefore supports the assumption made above. However, it is not clear altogether why the T dependency of H_0 should be a function of the H_0 *region*, and at very low values (e.g., −10), be quite strong. It is possible that the H_0 estimated values had a systematic inaccuracy due to difficulties in measuring pK_{BH^+} at elevated temperatures and I at concentrated acid. Indeed, as related to the latter point, researchers argued [23] that the extinction coefficient of B and BH^+ may be influenced by possible shifts in spectral absorption by the indicator accompanying changes in the medium that are not related to the acidity, as the acid concentration is changed.

Notwithstanding the apparent substantial effect of temperature on H_0 at high acidity, as obtained empirically from measurements related to the indicator, not the acid, we, in continuing the kinetic development of the present work to introduce the temperature dependence of H_0, chose to rely on the assumption that the Arrhenius effect on kinetic parameters is indeed considerably larger. The rationale for this, as related to the "ease of becoming protonated", is that concentrations (C) of the various species in Eq. (2) should change very little with temperature compared to the parallel change in activity coefficients, and the f_B/f_{BH^+} ratio is not expected to change significantly; as a result, the small change of pK_{BH^+} with T will be almost entirely offset by a change of similar magnitude, but with opposite sign, in $\log([B]/[BH^+])$ (see Eq. (3)).

Appendix B

B.1. $\varepsilon_{1/2\%}$ as acidity scale

On a $E_a/RT_{1/2\%}$ (=$\varepsilon_{1/2\%}$) scale,

$$\frac{E_a}{RT_{1/2\%}} = 2.3(H_0 + 23.4). \tag{B1}$$

The superacidity borderline of $H_0 = -12$ (100% H_2SO_4) corresponds to ($E_a/RT_{1/2\%}$ =) $\varepsilon_{1/2\%} = 26$. Values below 26 are then, by definition, those of superacids, whereas above 26 they represent "ordinary" acids, strong and weak. A H_0–$\varepsilon_{1/2\%}$ correlation chart is given in Table B1 and a corresponding correlation scale, in Fig. B1. As seen in Fig. B1, the approximate (practical) range of superacids is 26–8 on the $\varepsilon_{1/2\%}$ scale (H_0, −12 to −20), the range of strong acids is 40–26 (−6 to −12), and the range of weak acids, 55–40 (0.5 to −6).

Clearly, the $\varepsilon_{1/2\%}$ scale does not come to *replace* the H_0 scale, and it is a specific scale based on catalytic studies done under well-defined, strict conditions. However, it is convenient to use this scale when the isobutane conversion test is performed to rank catalysts for their acidity strength. This is especially convenient as the test provides a "continuous" scale, whereas Hammett acidity measurements (by the visual method) are incremental as they involve indicators of given pK_a's; no value can be obtained between successive indicators unless measurements are performed at different concentrations using a spectrophotometer or colorimeter [18], making the test (indicators) tedious and impractical for simple application. In the isobutane test, catalysts can be distinguished even if in the indicator measurements (based on color change) they give the same strength, say between −12.4 and −13.7. In addition, the indicator method is difficult to run smoothly (see above). One has to be especially careful to not allow humidity to interfere – a problem especially affecting the measurement of superacid solids – and the method is impossible with solids that are not completely colorless. Thus, for verifying the value of $Int_{1/2\%}$ under given conditions (that may differ from the ones in the literature), we may obtain $\varepsilon_{1/2\%}$ ($E_a/RT_{1/2\%}$) and H_0 values for one or two "standards", then apply the isobutane test (HAT) to any other solid acid and present the result on the $\varepsilon_{1/2\%}$–H_0 correlation scale. Otherwise, we may perform a one-on-one comparison of two catalysts for which we measured $\varepsilon_{1/2\%}$, when one ("standard") has a known H_0 value. Then, from the above, it is obvious that

$$H_0(2) = 0.4343[\varepsilon_{1/2\%}(2) - \varepsilon_{1/2\%}(1)] + H_0(1). \tag{B2}$$

For example, for catalyst (1) being "LZ-Y210(6) [2.0]" with $\varepsilon_{1/2\%}$ = 28.24 and $H_0 = -10.0$ [11], and catalyst (2) being SZ with $\varepsilon_{1/2\%}$ = 11.3 [14], we can calculate H_0(SZ) as follows:

$$H_0(SZ) = 0.4343 \times (11.3 - 28.24) - 10.0 = -17.35.$$

Table B1
H_0–$\varepsilon_{1/2\%}$ correlation chart.

H_0	$\varepsilon_{1/2\%}$	$\varepsilon_{1/2\%}$	H_0
0.0	53.8	55.0	0.5
−1.0	51.5	52.5	−0.6
−2.0	49.2	50.0	−1.7
−3.0	46.9	47.5	−2.7
−4.0	44.6	45.0	−3.8
−5.0	42.3	42.5	−4.9
−6.0	40.0	40.0	−6.0
−7.0	37.7	37.5	−7.1
−8.0	35.4	35.0	−8.2
−9.0	33.1	32.5	−9.3
−10.0	30.8	30.0	−10.4
−11.0	28.5	27.5	−11.4
−12.0	26.2	25.0	−12.5
−13.0	23.9	22.5	−13.6
−14.0	21.6	20.0	−14.7
−15.0	19.3	17.5	−15.8
−16.0	17.0	15.0	−16.9
−17.0	14.7	12.5	−18.0
−18.0	12.4	10.0	−19.1
−19.0	10.1	7.5	−20.1
−20.0	7.8	5.0	−21.2

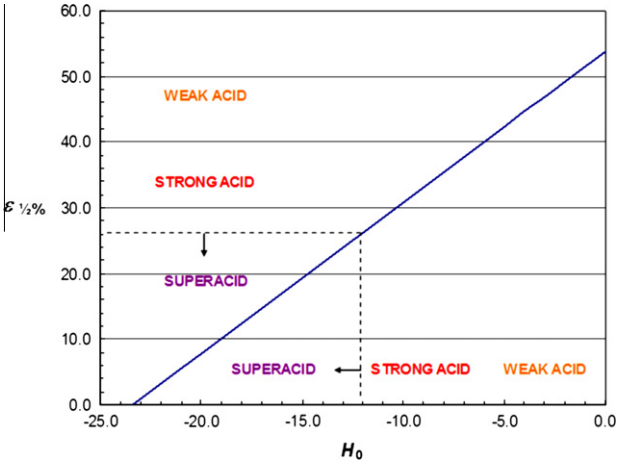

Fig. B1. H_0–$\varepsilon_{1/2\%}$ correlation scale.

References

[1] R.J. Gillespie, T.E. Peel, Adv. Phys. Org. Chem. 9 (1971) 1.
[2] G.A. Olah, G.K. Surya Prakash, Á. Molnár, J. Sommer, Superacid Chemistry, second ed., Wiley, 2009.
[3] M. Hino, K. Arata, J. Chem. Soc. Chem. Commun. (1980) 851.
[4] K. Arata, Appl. Catal. A 146 (1996) 3.
[5] T. Riemer, D. Spielbauer, M. Hunger, G.A.H. Mekhemer, H. Knözinger, J. Chem. Soc. Chem. Commun. (1994) 1181.
[6] L.M. Kustov, V.B. Kazansky, F. Figueras, D. Tichit, J. Catal. 150 (1994) 143.
[7] V. Adeeva, J.W. de Haan, J. Janchen, G.D. Lei, V. Schunemann, L.J.M. van de Ven, W.M.H. Sachtler, R.A. van Santen, J. Catal. 151 (1995) 364.
[8] R.S. Drago, N. Kob, J. Phys. Chem. B 101 (1997) 3360.
[9] Z. Hong, K.B. Fogash, R.M. Watwe, B. Kim, B.I. Masqueda-Jimenez, M.A. Natal-Santiago, J.M. Hill, J.A. Dumesic, J. Catal. 178 (1998) 489.
[10] B.S. Umansky, W.K. Hall, J. Catal. 124 (1990) 97.
[11] B. Umansky, J. Engelhardt, W.K. Hall, J. Catal. 127 (1991) 128.
[12] G.B. McVicker, G.M. Kramer, J.J. Ziemiak, J. Catal. 83 (1983) 286.
[13] D. Fărcaşiu, A. Ghenciu, J.Q. Li, J. Catal. 158 (1996) 116 (and references therein).
[14] D. Fraenkel, Chem. Lett. (1999) 917.
[15] K. Arata, H. Matsuhashi, M. Hino, H. Nakamura, Catal. Today 81 (2003) 17.
[16] D. Fraenkel, 21st North America Catalysis Society Meeting, San Francisco, CA, USA, Paper OA59, 2009.
[17] W.K. Hall, J. Engelhardt, G.A. Sill, in: P.A. Jacobs, R.A. van Santen (Eds.), Zeolites: Facts, Figures, Future, Elsevier, Amsterdam, 1989, p. B-1253.
[18] L.P. Hammett, A.J. Deyrup, J. Am. Chem. Soc. 54 (1932) 2721.
[19] C. Walling, J. Am. Chem. Soc. 72 (1950) 1164.
[20] H.A. Benesi, J. Am. Chem. Soc. 78 (1956) 5490.
[21] H.A. Benesi, B.H.C. Winquist, in: D.D. Eley, H. Pines, P.B. Weisz (Eds.), Advances in Catalysis, vol. 27, Academic Press, New York, 1978, p. 97.
[22] D. Fraenkel, 14th North American Meeting of the Catalysis Society, Snowbird, Utah, Paper T-48, 1995.
[23] M.A. Paul, F.A. Long, Chem. Rev. 57 (1957) 1;
F.A. Long, M.A. Paul, Chem. Rev. 57 (1957) 935.
[24] J. Sommer, R. Jost, Pure Appl. Chem. 72 (2000) 2309.
[25] W.G. Appleby, W.H. Avery, W.K. Meerbott, J. Am. Chem. Soc. 69 (1947) 2279.
[26] D. Fraenkel, Catal. Lett. 58 (1999) 123.
[27] D. Fraenkel, Ind. Eng. Chem. Res. 36 (1997) 52.
[28] Y.W. Bizreh, B.C. Gates, J. Catal. 88 (1984) 240.
[29] H. Pines, The Chemistry of Catalytic Hydrocarbon Conversions, Academic Press, New York, 1981.
[30] J. Engelhardt, G. Onyestyak, W.K. Hall, J. Catal. 157 (1995) 721.
[31] G.A. Olah, J. Org. Chem. 66 (2001) 5943.
[32] D.J. Parrillo, R.J. Gorte, W.E. Farneth, J. Am. Chem. Soc. 115 (1993) 12441.
[33] W.E. Farneth, R.J. Gorte, Chem. Rev. 95 (1995) 615.
[34] D.H. Aue, H.M. Webb, M.T. Bowers, J. Am. Chem. Soc. 98 (1976) 318.
[35] D.H. Aue, M.T. Bowers, in: M.T. Bowers (Ed.), Gas Phase Ion Chemistry, vol. 2, Academic Press, New York, 1979, p. 1 (Chapter 9).
[36] D.J. Parrillo, R.J. Gorte, J. Phys. Chem. 97 (1993) 8786.
[37] G. Yaluris, R.B. Larson, J.M. Kobe, M.R. González, K.B. Fogash, J.A. Dumesic, J. Catal. 158 (1996) 336.
[38] E.H. Teunissen, R.A. van Santen, A.P.J. Jansen, F.B. van Duijneveldt, J. Phys. Chem. 97 (1993) 203.
[39] B.-Q. Xu, W.M.H. Sachtler, J. Catal. 165 (1997) 231.
[40] V.M. Mastikhin, A.V. Nosov, S.V. Filimonova, V.V. Terskikh, N.S. Kotsarenko, V.P. Shmachkova, V.I. Kim, J. Mol. Catal. A: Chem. 101 (1995) 81.
[41] M.R. González, J.M. Kobe, K.B. Fogash, J.A. Dumesic, J. Catal. 160 (1996) 290.
[42] E. Cremer, Adv. Catal. 7 (1955) 75.
[43] D.M. Brouwer, in: R. Prins, G.C.A. Schuit (Eds.), Chemistry and Chemical Engineering of Catalytic Processes, Sijthoff & Noordhoff, Alphen aan den Rijn, 1980, p. 137.
[44] D.M. Brouwer, J.A. van Doorn, Rec. Trav. Chim. 90 (1971) 535.
[45] R. Jost, J. Sommer, Rev. Chem. Intermediat. 9 (1988) 171.
[46] G.A. Olah, R.H. Schlosberg, J. Am. Chem. Soc. 90 (1968) 2726.
[47] G.A. Olah, O. Farooq, A. Husain, N. Ding, N.J. Trivedi, J.A. Olah, Catal. Lett. 10 (1991) 239.
[48] H.S. Harned, B.B. Owen, The Physical Chemistry of Electrolytic Solutions, third ed., Reinhold Publishing Corp., New York, 1958.
[49] D. Fraenkel, Mol. Phys. 108 (2010) 1435.
[50] H. Otouma, Y. Arai, H. Ukihashi, Bull. Chem. Soc. Jpn. 42 (1969) 2449.
[51] M. Ikemoto, K. Tsutsumi, H. Takahashi, Bull. Chem. Soc. Jpn. 45 (1972) 1330.
[52] H.A. Benesi, J. Catal. 8 (1967) 368.
[53] B.W. Burbridge, I.M. Keen, M.K. Eyles, Adv. Chem. Ser. 102 (1971) 400.
[54] H. Pfeifer, D. Freude, J. Kärger, in: G. Öhlmann et al. (Eds.), Catalysis and Adsorption by Zeolites, Elsevier, Amsterdam, 1991, p. 89.
[55] H. Armendariz, C. Sanchez Sierra, F. Figueras, B. Coq, C. Mirodatos, F. Lefebvre, D. Tichit, J. Catal. 171 (1997) 85.
[56] J.F. Haw, J. Zhang, K. Shimizu, T.N. Venkatraman, D.-P. Luigi, W. Song, D.H. Barich, J.B. Nicholas, J. Am. Chem. Soc. 122 (2000) 12561.
[57] J.F. Haw, J.B. Nicholas, T. Xu, L.W. Beck, D.B. Ferguson, Acc. Chem. Res. 29 (1996) 259.
[58] J.B. Nicholas, J.F. Haw, L.W. Beck, T.R. Krawietz, D.B. Ferguson, J. Am. Chem. Soc. 117 (1995) 12350;
T. Xu, E.J. Munson, J.F. Haw, J. Am. Chem. Soc. 116 (1994) 1962;
T. Xu, J.F. Haw, J. Am. Chem. Soc. 116 (1994) 10188.
[59] J.F. Haw, Phys. Chem. Chem. Phys. 4 (2002) 5431.
[60] K.B. Fogash, R.B. Larson, M.R. González, J.M. Kobe, J.A. Dumesic, J. Catal. 163 (1996) 138.
[61] V. Adeeva, H.-Y. Liu, B.-Q. Xu, W.M.H. Sachtler, Topics Catal. 6 (1998) 61.
[62] F. Garin, L. Seyfried, P. Girard, G. Maire, A. Abdulsamad, J. Sommer, J. Catal. 151 (1995) 26.
[63] M. Guisnet, Acc. Chem. Res. 23 (1990) 392.
[64] C. Bearez, F. Avendano, F. Chevalier, M. Guisnet, Bull. Soc. Chim. Fr. 5 (1985) 346.
[65] C.D. Johnson, A.R. Katritzky, S.A. Shapiro, J. Am. Chem. Soc. 91 (1969) 6654.
[66] P. Tickle, A.G. Briggs, J.M. Wilson, J. Chem. Soc. (B) (1970) 65.